ACS Catalysis

Review

pubs.acs.org/acscatalysis

Shaped Carbons As Supports for the Catalytic Conversion of Syngas to Clean Fuels

Haifeng Xiong,*[,†,∥] Linda L. Jewell,[‡] and Neil J. Coville*[,†,§]

[†]DST-NRF Center of Excellence in Strong Materials and Molecular Sciences Institute, School of Chemistry, [§]DST-NRF Center of Excellence in Catalysis and Molecular Sciences Institute, School of Chemistry, University of the Witwatersrand, Private Bag X3, Braamfontein, Johannesburg 2050, South Africa

[‡]DST-NRF Center of Excellence in Catalysis and Department of Chemical Engineering, University of South Africa, P/Bag X6, Florida, Johannesburg 1710, South Africa

[∥]Department of Chemical & Biological Engineering and Center for Microengineered Materials, University of New Mexico, Albuquerque, New Mexico 87131, United States

ABSTRACT: The conversion of syngas to hydrocarbons via Fischer−Tropsch synthesis (FTS) and to alcohols via higher alcohols synthesis (HAS) are two important chemical reactions that generate liquid fuels. Heterogeneous catalysts supported on carbon have been used in both of these fields. In this review, we first describe the features and surface properties of several shaped carbon materials, including carbon black, activated carbon, carbon nanotubes, carbon nanofibers, carbon spheres, ordered mesoporous carbon, graphene, and diamond. In particular, the microscopic structures of these shaped carbons are compared to differentiate the specific characteristics of different shaped carbons. Then we review the recent advances in the study of heterogeneous catalysts supported on these shaped carbon materials used for FTS and HAS from syngas in the past two decades. Various catalyst parameters, such as promoters, stability, autoreduction, pore structure, carbon morphology, and metal particle size, etc., are discussed and summarized.

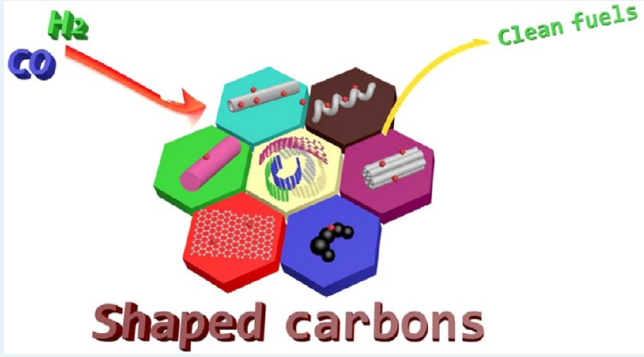

KEYWORDS: *shaped carbons, syngas, Fischer−Tropsch synthesis, higher alcohols synthesis, catalysts, graphene*

1. INTRODUCTION

The finite petroleum resources available in the world have led to a re-evaluation of the production of alternative energy sources and the development of new energy utilization pathways that do not rely only on petroleum (even if oil prices have dropped in early 2015 below $60 per barrel). One reliable and well-known pathway for energy and fuel production is to combust biomass, natural gas, or coal to synthesis gas (syngas, CO/H_2), followed by the direct catalytic conversion of syngas to fuels and chemicals. Thus, the use of fuels that are produced from syngas as an energy source provides an important alternative to at least partly supplement energy demand from crude oil. In this process, the syngas-to-hydrocarbons (i.e., Fischer−Tropsch synthesis, FTS, eqs 1 and 2) or -to-alcohols (eq 3) routes are two important chemical reactions that generate liquid fuels. It should be noted that the FTS reaction generates mainly hydrocarbons, with minor formation of alcohols.[1] To generate high yields of long-chain alcohols to be used as fuels requires a change in catalyst formulation from that used in FTS; this process is referred to as higher alcohols synthesis (HAS).

$$n\mathrm{CO} + (2n+1)\mathrm{H_2} \rightarrow \mathrm{C}_n\mathrm{H}_{(2n+2)} + n\mathrm{H_2O} \quad (n \geq 1) \tag{1}$$

$$n\mathrm{CO} + 2n\mathrm{H_2} \rightarrow \mathrm{C}_n\mathrm{H}_{2n} + n\mathrm{H_2O} \quad (n \geq 1) \tag{2}$$

$$n\mathrm{CO} + 2n\mathrm{H_2} \rightarrow \mathrm{C}_n\mathrm{H}_{2n+2}\mathrm{O} + (n-1)\mathrm{H_2O} \quad (n \geq 1) \tag{3}$$

The conversion of syngas to hydrocarbons or to alcohols can be viewed, in principle, as a green process because it entails a catalytic reaction in which all the carbon in CO is converted to CH_x/CH_xOH species and the H is converted to water. The FTS and HAS processes are surface-catalyzed reactions involving chain growth and termination of carbon fragments, generated from the hydrogenation of adsorbed CO over a catalyst. Although commercial FTS catalysts (based on iron and cobalt) are well-known, alcohol synthesis to make fuels *directly* from syngas has not been well-established in industry.[2] This, of course, excludes the formation of MeOH from syngas, a well-known industrial process; once made, the MeOH can be *indirectly* converted into long chain hydrocarbon fuels.

Received: January 17, 2015
Revised: March 9, 2015
Published: March 10, 2015

DOI: 10.1021/acscatal.5b00090
ACS Catal. 2015, 5, 2640−2658

Control of the products in FTS and HAS is influenced by many factors that include reactor design, process variables, and the nature of the catalyst.[3] Because most industrial catalysts are typically supported on a porous material, the physical and chemical properties of the support can impact FTS and HAS selectivity and activity. Indeed, supports have been found to significantly affect the catalyst performances in FTS and HAS. Compared with conventional oxide supports, such as Al_2O_3, SiO_2, and TiO_2, carbon supports are attractive because they display a relatively weak interaction between the metal and the carbon, and this allows for the easy tailoring of the catalyst properties by modification of the chemical and physical characteristics of the carbon. Carbon materials with different morphologies, such as carbon black, activated carbon, glassy carbon, and carbon nanofibers, have been successfully used in FTS for decades.

More recently, a new generation of carbon materials have been synthesized via carbonization of solids, liquids, or gases.[4,5] These new materials contain carbon atoms that have a mix of sp^2 and sp^3 orbitals, and it is both the ratio of these orbitals and the curvature associated with sp^2–sp^2 bonding patterns that give rise to myriad new structures that have not been synthesized prior to 1992.

Early studies (pre-1992) on carbon supported catalysts for use in FTS and HAS mainly focused on carbon black, glassy carbon, and activated carbon as supports.[6,7] In the past two decades, there has been an ever-increasing interest in the use of new carbon materials, with uniform structures, for use in syngas conversion; however, a systematic approach to aid understanding of the effect of the different carbon morphologies on the syngas conversion reactions is still to be realized.

In this review, we have summarized recent advances in the conversion of syngas to hydrocarbons and to alcohols using heterogeneous catalysts supported on differently shaped carbon materials, including carbon black, activated carbon, carbon nanotubes, carbon nanofibers, graphene oxide, carbon spheres, mesoporous carbon, diamond, and heteroatom-doped carbons. The issue of hierarchical carbons mixed with other supports in which the primary FT or HAS products are further converted into fuels will be briefly described.[8] It is also to be noted that a number of important reviews have appeared on carbon supports in the past few years that have included the issue of FT to varying degrees.[9−13] Our review has focused on the general relationship of the carbon catalyst structure to performance in both the FTS and HAS processes.

This Review is divided into six sections: Section 1 is the Introduction. In section 2, the preparation and structure of the shaped carbon materials is described. Due to the hydrophobic nature of the surface of most carbon materials, it is necessary to activate the carbon surface and make the surface hydrophilic. In the third section, the physical and chemical surface properties of these new and old shaped carbon materials are described. In the fourth section, the catalyst performances in FTS of the catalysts supported on shaped carbon materials is reviewed. The use of carbon-supported catalysts in HAS from syngas is described in the fifth section. The last section provides some conclusions and perspectives on this active field. This paper thus provides an overview of catalysts supported on shaped carbon materials for the direct conversion of syngas into hydrocarbon and higher alcohols based fuels.

2. PREPARATION AND STRUCTURAL FEATURES OF SHAPED CARBON MATERIALS

2.1. Carbon Black. Carbon black (CB) has been produced both intentionally and unintentionally for millennia. Nowadays, in addition to its use in the tire industry (over 90%), CB has been used in pigmentations, industrial rubber products, plastics and printing inks, conductive agents and batteries, etc.[14]

CB is a carbonaceous material produced in industry by the incomplete combustion of heavy petroleum products (such as tar) or by the thermal decomposition of gaseous or liquid hydrocarbons. It is a form of para-crystalline carbon that has a high surface area to volume ratio and is composed of fine carbon particles, which are usually found in a bead-like (accreted) cluster arrangement (Figure 1). CBs are commercially available from

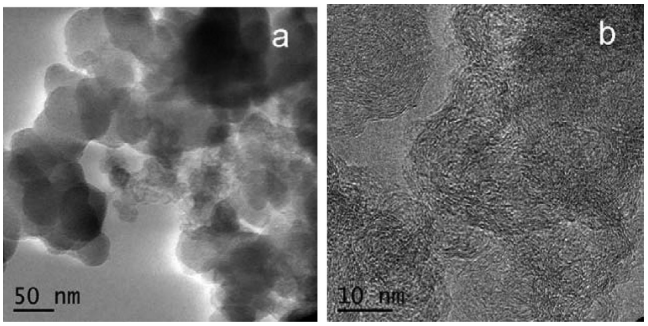

Figure 1. Representative TEM images of carbon black: (a) low magnification; (b) high magnification showing its graphitic structure. Adapted from ref 16 (Xiong, H.; Wang, T.; Shanks, B.; Datye A. Tuning the Location of Niobia/Carbon Composites in a Biphasic Reaction: Dehydration of D-Glucose to 5-Hydroxymethylfurfural. *Catal. Lett.* **2013**, *143*, 509−516.) with kind permission from Springer.

many companies, with a wide range of surface areas and porosities, ranging from nonporous, highly ordered, and homogeneous particles to highly porous aggregates with surface areas up to 1500 $m^2\ g^{-1}$. CB, based on annual tonnage, is one of the top 50 industrial chemicals manufactured worldwide. The detailed production and applications of carbon black can be found in Donnet et al.[15]

2.2. Activated Carbon. Activated carbon (AC) is "porosity enclosed by carbon atoms, which has the size of molecules and is slit-shaped".[17] There are several hundred activated carbons available commercially, all with different porosity for use in specific applications and typically made from different source materials. However, different activated carbons with different properties can also be made from one source material. A generally accepted model of AC can be represented in a cartoon that shows a representative structure consisting of aromatic sheets and strips (Figure 2 (a)). These are typically bent and the overall picture corresponds to that of crumpled paper, with the gaps between the sheets or parts of sheets representing micropores (Figure 2(b)). All the ACs have a porous structure but they also contain some chemically bonded heteroatoms (mainly oxygen and hydrogen). Thermal decomposition of ACs in air always leaves a residue (ca. 15% ash). This ash typically contains silica and other oxides (the nature and amount is a function of the precursor).

Activated carbons are used mainly for the purification of water and air and the separation of gas mixtures. Only a few resources are used for activated carbon production, including coals, peat, and woods as well as some synthetic organic polymers. The key

DOI: 10.1021/acscatal.5b00090
ACS Catal. 2015, 5, 2640−2658

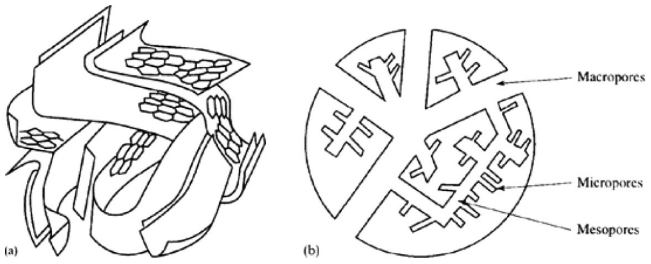

Figure 2. Schematic representation of the structure of (a) activated carbon and (b) an activated carbon granule. Reprinted from ref 18 (Rodríguez-Reinoso, F. The role of carbon materials in heterogeneous catalysis. *Carbon*, **1998**, *36*, 159−175); copyright 2014, with permission from Elsevier.

features are the reliability and consistency of the resource. Glassy carbons are considered as a type of activated carbon with slit-shaped pores and have also been referred to as carbon molecular sieves.[18] The detailed application and properties of ACs can be found in a book by Marsh and Rodriguez-Reinoso.[17]

2.3. Carbon Nanofibers. Carbon nanofibers (CNFs) were first prepared over a century ago.[19,20] A key feature found in all CNFs is that they are made of domains of sp^2 carbon atoms (graphene-like layers) bounded by sp^3 carbons or other terminal atoms or groups of atoms. Cartoon structures of some typical CNFs are shown in Figure 3. Figures 3a−c show the platelet,

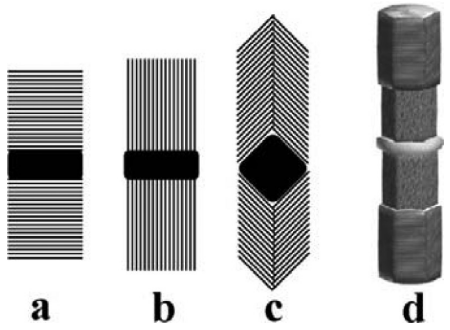

Figure 3. Illustration of different types of carbon nanofibers (CNFs): (a) platelet fibers; (b) ribbonlike fibers; (c) herringbone fibers; and (d) coblock carbon nanofibers; adapted from ref 4.

ribbonlike and herringbone (or fishbone) structure of fibers that are made from graphene layers. The synthesis and application of graphene-domained CNFs have been well described elsewhere.[19]

When CNFs are made in low-tempertaure processes, there is much less graphitic carbon detected; that is, more sp^3 bonding is noted. The actual morphology of the CNFs is determined by the carbon source (keeping the catalyst and reaction conditions the same).[4] This allows for the generation of so-called "coblock" CNFs to be made by generating a CNF by sequentially using two or more different carbon sources, as seen in the cartoon shown in Figure 3d.[4]

2.4. Carbon Nanotubes. Carbon nanotubes (CNTs) have a unique nanostructure that gives their remarkable electronic and mechanical properties;[11] however, only the multiwalled CNTs (MWCNTs) have been studied in depth as catalyst supports. MWCNTs do not have the perfect 1-D linear structures shown in most cartoon representations of the material but typically have a wavy structure (think of cooked spaghetti rather than raw spaghetti) and have a rough surface (Figure 4).[21] Of importance in terms of CNT morphology is the parallel arrangement of the

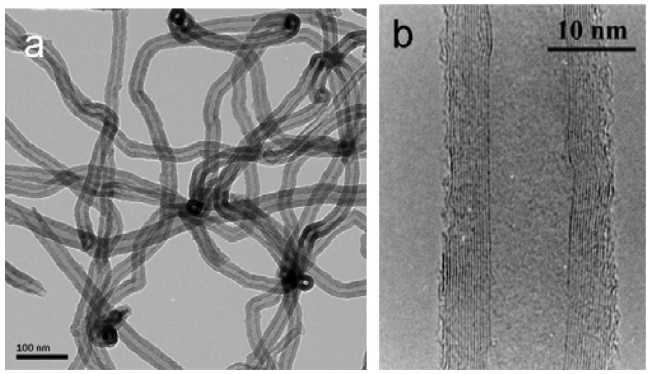

Figure 4. Representative TEM images of CNTs: (a) low magnification; (b) high magnification. Adapted from ref 24.

graphene layers along the tube axis and the generation of the cavity in the tube.[22] As-produced MWCNTs typically have surface areas ranging between 50 and 400 m^2/g. They typically have no micropores, and the mesopore volume (determined by the diameter of the tube) ranges between 0.5 and 2 mL/g. They are now commercially available from many suppliers.

It should be noted that it is easy to confuse MWCNTs with CNFs. For example, they are both one-dimensional carbon materials and can be prepared by similar procedures.[5,23] Both CNFs and MWCNTs are believed to grow by decomposition of an organic reactant on a catalyst particle. The carbon atoms then move over or through the catalyst, followed by crystallization of the carbon on the catalyst surface.[19] However, recent studies have suggested that the synthesis of CNFs and CNTs, especially at low temperatures, may occur by a surface diffusion mechanism. The detailed differences and similarities in electronic, adsorption, mechanical and thermal properties, and growth mechanisms have been reviewed.[19,20] Some physical features associated with CNTs and CNFs used in syngas conversion are shown in Table 1.

2.5. Carbon Microcoils. Carbon microcoils (CMCs), or helical carbon, are another member of the nanostructured carbon materials.[44] The CMCs are a polymer-like carbon that has a

Table 1. Typical Features of Carbon Nanofibers and Nanotubes Used in Syngas Conversion

	structure feature			
carbon materials	BET surface area (m^2/g)	pore volume (cm^3/g)[a]	diameter (nm)[b]	ref
CNFs	137−194	0.21−0.38	30	25−28
	276	0.46	6.7	29
	3.8	N.A.	N.A.	30
	123−164	0.29−0.51	5.5−10.9	31
	93	0.19	9.2	32
CNTs	80	0.3	9	33, 34
	109	N.A.	N.A.	35
	212; 218	0.58; 0.55	8−12; 20−50	36
	29	0.086	40−80	37
	N.A.	N.A.	2−12	38, 39
	N.A.	4	10−20	40
	72−164	0.36−0.74	10−50	41
	N.A.	N.A.	3−5	42
	198−285	0.44−0.7	N.A.	43

[a]N.A.= not available. [b]For CNFs, the exterior diameter was measured, and for CNTs, the interior diameter was measured.

DOI: 10.1021/acscatal.5b00090
ACS Catal. 2015, 5, 2640−2658

corkskrew-like structure made up of carbon atoms containing significant sp^3 hybridization. The CMCs are poorly graphitic. CMCs are different from conventional CNFs and can have different thermal stability and carbon atom arrangements.[45] Thus, these materials allow for the study of the impact of sp^3 bonding on the catalytic activity of carbon supports. Carbon microcoils are typically prepared using Cu or Ni catalysts by CVD at low temperatures (<300 °C) (Figure 5).[46] The detailed applications and properties of CMCs can be found in a recent review.[47]

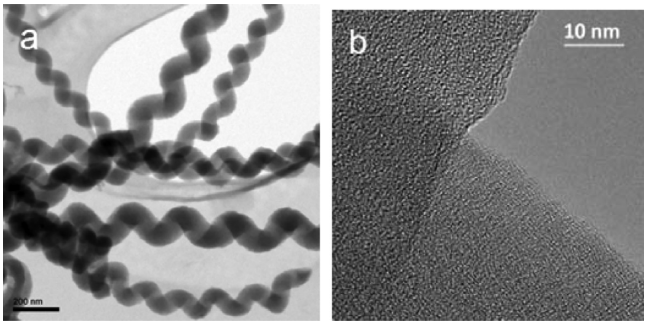

Figure 5. Representative TEM images of carbon microcoils: (a) low magnification TEM image showing their spring-like structure; (b) higher magnification TEM image of CMCs showing their amorphous structure. Reprinted from ref 45 (Xiong, H.; Motchelaho, M. A. M.; Moyo, M.; Jewell L. L.; Coville, N. J. Cobalt catalysts supported on a microcoil carbon in Fischer−Tropsch synthesis: A comparison with CNTs and CNFs. *Catal. Today*, **2013**, *214*, 50−60); copyright 2014, with permission from Elsevier.

Coiled carbon tubes are also known.[48] These, as the name implies, are like CNTs with graphitic walls parallel to the tube axis. To date, they have not been explored as catalyst supports.

2.6. Carbon Spheres (CSs). Carbon spheres (CSs) is the generic name given to carbons that have been made from a carbon source in the absence of O_2 and require no catalyst. They have been given many other names, including carbon balls, carbon nanospheres, carbon microbeads, onions, etc.[49] There are two major approaches used for the synthesis of carbon spheres. One is the CVD method involving the high-temperature decomposition of a carbon reactant, typically in the absence of a catalyst. These CSs require no purification to remove residual metal catalyst as found in CNTs and CNFs. The surface of these CSs prepared by CVD is composed of random curling graphitic flakes with sizes ranging from 1 to 10 nm. If these flakes are tightly packed, they produce CSs with low surface areas (<10 m^2/g). When very small CSs (called onions) are produced, their surface consists of nearly complete graphite layers.

The second method used to make CSs is hydrothermal synthesis (HTS).[50,51] The CSs prepared by HTS are usually derived from the carbonization of an organic carbon precursor, such as glucose or sucrose, in an autoclave. The structure and formation mechanism of these CSs is not well understood.[52]

Representative SEM/TEM images of CSs are shown in Figure 6. Methods to achieve synthesis, doping, functionalization, and application of carbon spheres can be found in a chapter by Titirici[51] and reviews.[53,54]

2.7. Ordered Mesoporous Carbon. Ordered mesoporous carbons (OMCs) are materials that have a repetitive porous structure in the nanometer range (Figure 7). The OMCs are made by covering a template with an appropriate carbon reactant. Templates are classified as hard or soft.[57] A hard

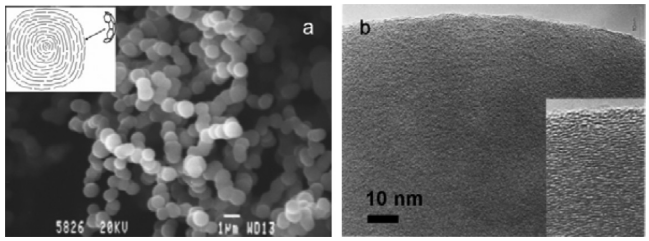

Figure 6. Representative SEM and TEM images of carbon spheres (CSs): (a) SEM image of carbon spheres and cartoon illustration of a carbon sphere prepared by CVD (insert), Reprinted from ref 55 (Xiong, H.; Moyo, M.; Motchelaho, M. A. M.; Jewell, L. L.; Coville, N. J. Fischer−Tropsch synthesis over model iron catalysts supported on carbon spheres: The effect of iron precursor, support pretreatment, catalyst preparation method and promoters. *Appl. Catal., A* **2010**, *388*, 168−178); copyright 2014, with permission from Elsevier; (b) HRTEM image of a carbon sphere showing that the sphere is composed of graphitic layers, with the *c*-axis approximately parallel to the radial direction. The inset is a magnified region. Reprinted from ref 56 (Wang, Z. L.; Kang, Z.C. Pairing of pentagonal and heptagonal carbon rings in the growth of nanosize carbon spheres synthesized by a mixed-valent oxide-catalytic carbonization process. *J. Phys. Chem.* **1996**, *100*, 17725−17731); copyright 2014, American Chemical Society.

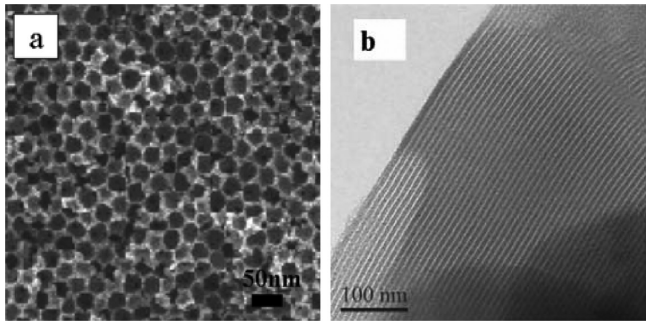

Figure 7. Representative SEM/TEM images of mesoporous carbon materials (a) with pore size of 25 nm synthesized using colloidal silica particles as templates and (b) synthesized using SBA-15 as the template. Reprinted with permission from ref 61 (Chai,G. S.; Yoon, S. B.; Yu, J.-S.; Choi, J.-H.; Sung, Y.-E. *J. Phys. Chem. B* **2004**, *108*, 7074−7079); copyright 2014, American Chemical Society.

template is made from a presynthesized organic or inorganic template,[58] and the soft template method generates a nanostructured carbon through co-condensation and carbonization.[59,60] The corresponding pore structures are determined by synthetic conditions, such as mixing ratios, solvents, and temperatures. The detailed synthesis of mesoporous carbons can be found in a review by Liang et al.[57] OMCs are used as supports in catalysis because they show improved mass transport of molecules compared with microporous carbons.

2.8. Graphene, Graphite, and Diamond. Graphene is a one-dimensional material with one or several layers of stacked sheets of sp^2-hybridized carbon in which the number of sheets does not exceed 10 (Figure 8a).[62] Oxidation of graphene leads to a surface rich in O atoms. Reduction of this graphene oxide gives reduced graphene oxide, which can be used as a catalyst support. Beyond 10 layers, graphite occurs in a stacked hexagonal structure with an interlayer spacing of 3.34 Å, the van der Waals distance for sp^2-bonded carbon (Figure 8b). There are several types of graphite, and they have very similar physical properties, except that the graphene layers stack slightly differently.

DOI: 10.1021/acscatal.5b00090
ACS Catal. 2015, 5, 2640−2658

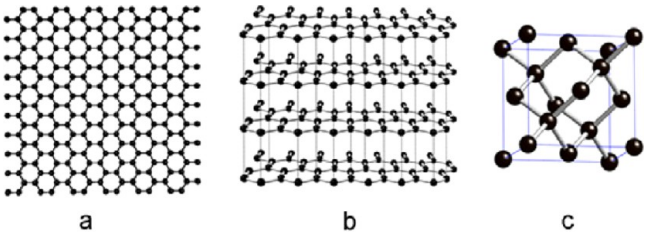

Figure 8. Schematic structure of (a) graphene, (b) graphite, and (c) a diamond crystal unit.

Diamond is a crystalline carbon material composed of sp^3 hybridized carbon atoms and is thus quite different from graphene-based carbon materials, which have substantial sp^2 hybridized carbon atoms. Diamond has long been considered a surface inert material (Figure 8c); however, oxidized diamond can be used to load active composites, which can be used in catalysis because the surface is rich in OH groups.[63,64]

2.9. Carbons with Other Shapes. Figure 9a shows an illustration of the structure of a fullerene. The fullerene molecule has a hollow structure and is composed entirely of carbon, with a spherical or ellipsoid shape. Fullerenes will need to be embedded in a matrix if used in heterogeneous catalysis.

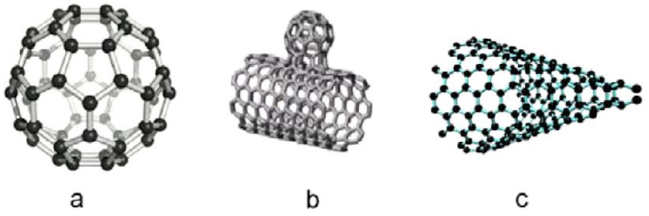

Figure 9. Cartoon illustrations of several carbons with novel shapes: (a) fullerene, (b) carbon buds, and (c) carbon horns.

Carbon materials with other shapes, such as carbon buds and horns (Figure 9b and c), have been made but rarely used in catalysis because of the difficulties of either their large-scale production or the purification of the carbons. A wide range of other carbons based on variations of the shapes mentioned have also been made. However, they have not been exploited in catalytic reactions.

3. SURFACE FUNCTIONALIZATION AND PROPERTIES OF THE SHAPED CARBONS

Raw carbon materials (i.e., the synthesized carbon prior to purification/functionalization) prepared by most procedures have hydrophobic surfaces, and it is difficult to prepare effective catalysts using these raw materials. If the carbons are not surface-activated, they cannot be properly dispersed in solvents. The limited defect sites on the carbon surface can also preclude a good metal−carbon support interaction. This can be overcome by doping (replacement of carbon atoms by noncarbon atoms) or by functionalization of the shaped carbon surface prior to the loading of an active metal. There are numerous methods that have been used to activate (i.e., functionalize) the shaped carbon surface, such as acid (liquid and gas) treatment,[65−67] base treatment,[65,68] oxidation and plasma treatment,[69] vacuum−ultraviolet photochemical reactions,[70] and microwave procedures.[71] However, the most efficient and lowest cost process is acid treatment.

3.1. Acid Treatment. Acid treatment of freshly synthesized shaped carbons creates adsorption sites on the surface of the shaped carbons needed for anchoring metal precursors. The generation of CNTs as a support occurs in two steps:[72] The first step involves the removal of the catalyst required to make the CNT,[73−75] and in the second step, a strong oxidative medium is used to remove amorphous carbon and roughen the CNT surface.

There are different ways to purify and functionalize the carbon materials using acidic solutions, such as by treatment with nitric acid, concentrated sulfuric acid, aqua regia, $HF−BF_3$, aqueous OsO_4, or $KMnO_4$ (acid/alkali) solutions. Recently, a gas-phase route has been developed for the functionalization of CNTs.[66] The HNO_3 vapor treatment proved more effective for introducing oxygen-containing functional groups on CNT surfaces than a conventional treatment with liquid HNO_3, and it is more advantageous because the method avoids the filtration, washing, and drying steps.

3.2. Doping. Doping hybrid atoms into the nanostructures of shaped carbon is an alternative to increase the surface hydrophilicity and electrical conductivity of shaped carbon materials. The most extensively used dopants are nitrogen (N) and boron (B), which either add electrons to or subtract electrons from the carbon systems. When these hybrid carbon materials that have been doped with N or B are used in catalysis or electrochemistry, the electron donor and acceptor characteristic of the shaped carbon surface can be significantly affected and, thus, influence the reactive performance of a catalyst.[76] In this regard, nitrogen-doped carbon nanotubes (N-CNTs) have been found to be more metallic in behavior and exhibit strong electron donor states near the Fermi level.[77] Using tight-binding and ab initio calculations, pyridine-like N structures have been shown to be responsible for this metallic behavior.[77]

Two methods have been developed to dope shaped carbon materials: in situ doping and post doping. In in situ doping, the heteroatoms are introduced into the shaped carbon structure in one step during the preparation of the shaped carbon, whereas in the post doping method, the heteroatoms are introduced into the carbon structure by post-treatment after the shaped carbons have been prepared. A cartoon showing a comparison of the morphology of the nitrogen-doped carbon nanotubes (N-CNTs) prepared by either (a) in situ growth or (b) postdoping is illustrated in Figure 10.[78] N-CNTs prepared by the in situ growth method generally produce bamboo-like structures with the doped N atoms well dispersed both in the bulk and on the surface of the N-CNTs. In post doping, the doped N atoms tend to deposit only on the surface of the N-CNTs.[78]

3.3. Surface Properties. The surface properties of shaped carbon materials have been characterized by numerous techniques that include acid−base titration, zeta potential charge analysis, and X-ray photoelectron spectroscopy (XPS). For acid−base titration, selective neutralization at equilibrium with different bases of increasing strength is used to determine quantitatively the concentration of surface acidic groups.[45] The weakly acidic groups on the support surface are usually titrated using a strong base (NaOH), and the strongly acidic groups, such as carboxyls, are titrated using a very weak base ($NaHCO_3$).

Zeta potential measurements of CNTs can be used to determine the presence of oxygen-containing surface groups. The presence of acidic groups causes the carbon surface to be more hydrophilic, and this increases the negative surface charge density and, hence, decreases the pH of the point of zero charge (PZC). The PZC for a typical CNT occurs at pH = 4.9.[79,80] The

DOI: 10.1021/acscatal.5b00090
ACS Catal. 2015, 5, 2640−2658

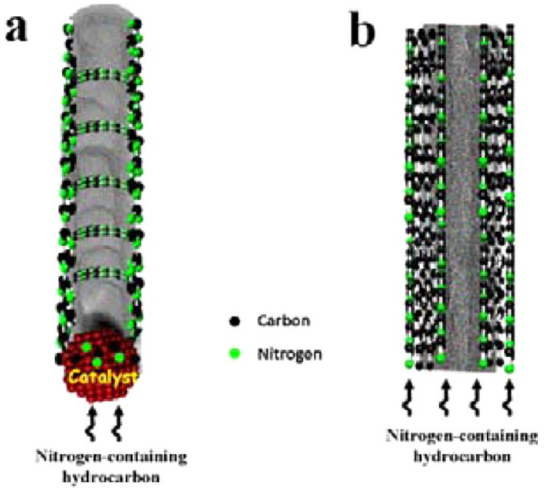

Figure 10. Cartoon illustrating the comparison of N doping by (a) in situ growth and (b) post doping for the preparation of nitrogen-doped carbon nanotubes.[78]

results of many studies using different experimental techniques indicate that there may be several types of oxygen functional groups formed on carbon surface, as shown in Figure 11.

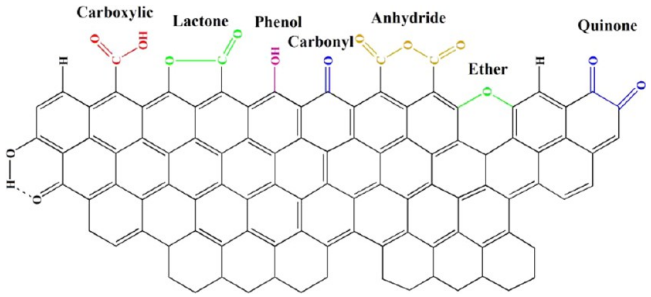

Figure 11. Surface containing oxygen groups on shaped carbon surface. Reprinted and modified from ref 81 (Figueiredo, J. L.; Pereira, M. F. R.; Freitas, M. M. A.; Órfão, J. J. M. Modification of the surface chemistry of activated carbons. *Carbon* **1999**, *9*, 1379−1389); copyright 2014, with permission from Elsevier.

3.4. Carbons as Catalyst Support. The use of carbons as supports has numerous advantages: (i) many different carbon materials can be purchased at reasonable prices; (ii) reclamation of the catalysts postreaction is possible by simply oxidising the carbon (surprisingly very few studies have been performed to exploit this property); (iii) the carbon surfaces can be modified by simple procedures (acidic, basic, oxidative). This makes the surfaces hydrophilic and also helps in dispersing the carbons in polar solvents during the catalyst loading process; (iv) doping of carbons by N atoms provides a facile means of generating small metal particles on a carbon surface; (v) although the above methods to dope/functionalize the carbons will affect their properties, the procedures appear to enhance their use as catalysts (e.g., reduced sintering) (see section 4).

Disadvantages include (i) the carbons can be oxidized at high temperatures, and this process can occur at lower temperatures in the presence of catalysts; (ii) the carbons can also be reduced to form CH_4, especially in the presence of catalysts; (iii) the mechanical robustness of many carbons has still to be tested; and (iv) the low density of many porous carbons.

4. SHAPED CARBON MATERIALS USED AS SUPPORTED FISCHER−TROPSCH SYNTHESIS CATALYSTS

4.1. Catalysts Supported on Activated Carbon, Carbon Black and Glassy Carbon. Early studies on carbon supported FTS catalysts focused on the use of activated carbon (AC), carbon black (CB), and glassy carbon as supports.[6,7,82−85] The focus in these studies was on the synthesis and use of small metal particles supported on carbon. These particles are easier to reduce than metal particles supported on metal oxides. The use of carbon, including activated carbon, carbon black, and glassy carbon, as a support was found to reduce the metal−support interaction and enhance metal oxide reduction.[18,83]

4.1.1. The Thermal Stability, Reduction and Promotion of Catalysts and Supports. AC; CB; and, to lesser extent, CNFs were the most commonly used carbon supports in FTS before 1992. These early studies focused on catalyst stability and metal−support interactions.

The thermal stability of the carbon supports was investigated under FTS conditions. When an Fe/activated carbon catalyst was reduced at 450 °C in H_2, the formation of ethane and propane in addition to methane and water was observed.[86] Tau and Bennett[7] reduced their Fe/CB catalyst in H_2 at 450 °C and observed the formation of H_2O, CO_2, CO, and CH_4. The AC- and CB-supported catalysts were not thermally stable under these reduction conditions. Mass loss was also observed during reduction in H_2 (350−450 °C) of an iron/glassy carbon, presumably because of support loss.[84] Rodríguez-Reinoso et al. have concluded that these carbon supports cannot be used in hydrogenation reactions above 427 °C or in the presence of oxygen above 227 °C because of gasification of the support.[18,87]

Catalyst reduction and, hence, the metal particle size were affected by the interaction between the metal and support. For CB-supported FT catalysts, Jung et al.[82] found that small Fe particles (1−2.7 nm) were more difficult to reduce than a catalyst with larger Fe particles, suggesting the existence of a metal−support interaction between iron and carbon. This interaction resulted in the formation of unreduced Fe^{2+} ions at low reduction temperatures in H_2;[88] however, the degree of reduction of the Fe/CB catalysts was higher than found for iron catalysts supported on silica or alumina.[6] Furthermore, it has been reported that reduction of all of the Fe in a catalyst prepared from $Fe_3(CO)_{12}$ on CB could be achieved at 200 °C in H_2.[89] Likewise, Fe−Co catalysts prepared from metal carbonyls on CB have been activated at 200 °C in H_2.[90]

The effect of the addition of several structural, reduction, and electron promoters on the catalytic performance of Fe/AC catalysts has been investigated. Ma et al. have found that promoters (K, Cu, Mo, Zr, and Ce) and the type of AC significantly affected the catalytic performance of Fe and Co catalysts in FTS.[91−93] They found that both FTS and WGS activities increased after the addition of 0.9 wt % K to a Fe/AC catalyst, whereas an opposite trend was observed with the addition of 2 wt % K.[91] The K promoter significantly shifted carbon selectivities to higher-molecular-weight hydrocarbons (C_5^+). The addition of a Cu promoter to a Fe/AC catalyst enhanced the reduction of iron significantly.[92] However, both FTS and WGS activities of the catalyst were lowered. The addition of 6% Mo into a Fe−Cu−K/AC catalyst improved catalyst stability without sacrificing activity, whereas the activity was suppressed dramatically on a 12% Mo-loaded catalyst.[93] The addition of Mo resulted in the production of more CH_4 and less

DOI: 10.1021/acscatal.5b00090
ACS Catal. 2015, 5, 2640−2658

Table 2. Carbon Properties, Reaction Conditions and Research Theme of Carbon Black and Activated Carbon Supported Catalysts Used in Fischer−Tropsch Synthesis (FTS)

		FTS conditions				
catalyst	support type and property	reduction	reaction	reaction parameter	performance[a,b]	ref
			Carbon Black			
Fe/CB	Columbia, T-10157	400 °C	0.1 MPa, 275 °C, H_2: CO = 1−9	porosity, stability	X = N.A., S_{5+} = 2−10%	83
Fe/CB	SA = 763 m^2/g	300 °C, 0.5 MPa	260−280 °C, 20 MPa, H_2/CO = 1	support effect, ozone treatment	X = 40−80%, S_{5+} = 60−80%	30
Fe/CB	Vulcan 3 (SA = 56 m^2/g)	400 °C	275 °C, 101 kPa, H_2/CO = 3	dispersion effect	X = 2.8−3.9%, S_{5+} = 5−12%	82
Ru/CB	V3G (62 m^2/g)	400 °C	190−250 °C 101 kPa H_2/CO=3	selectivity, interaction	X = 1.5−4.5%, S_{5+} < 1%	98
			Activated Carbon			
Fe/AC	from olive pits	400 °C	0.1 MPa, 275 °C, H_2/CO = 3	porosity, stability	X = 2−27%, S_{5+} = 2−10%	83
Fe−K/AC, Fe−Cu/AC,	Sigma-Aldrich	400 °C, 0.5 MPa	280 °C, 300 psig, H_2/CO = 0.9	Cu promoter effect	X = 28−85%, S_{5+} = 50−61%	92
Fe−Mo−Cu-K/AC	from peat, generic wood, pecan, walnut	400 °C, 0.5 MPa	290 °C, 300 psig, H_2/CO = 0.9	K promoter, AC nature effects	X = 29−97%, S_{5+} = 16−62%	91, 95
Fe/AC	SA = 1170 m^2/g	300 °C, 0.5 MPa	260−280 °C, 2.0 MPa, H_2/CO = 1	support effect, ozone treatment	X = 40−80%, S_{5+} = 60−80%	30
Co/AC	N.A.	400 °C	220−250 °C, 2−4 MPa, H_2/CO = 1.0−2.5	product distribution, kinetics	X = 10−54%, S_{5+} = N.A.	99, 100
Zr−Co/AC La−Zr−Co/AC	SA=1068.7 m^2/g PV=0.65 cm^3/g	400 °C	250 °C, 2.5 MPa, H_2/CO = 2	lanthanum promoter	X = 49−93%, S_{5+} = 63−75%	101, 102
ZSM-5-Fe/AC	Norit SX Ultra (Sigma-Aldrich)	1 atm, 400 °C	280−320 °C, 300 psig, H_2/CO = 1	zeolite promoter	X = 70−90%, S_{5+} = N.A.	103, 104
Fe−Cu−K/AC	Sigma-Aldrich	0.5 MPa, 400 °C	310−320 °C, 2.2 MPa, H_2/CO = 0.9	Mo promoter, reducibility	X = N.A., S_{5+} = 39−52%	93

[a] X stands for the CO conversion and S_{5+} stands for the C_{5+} hydrocarbon selectivity. [b] N.A. = not available.

C_5^+ hydrocarbons. Because of a strong interaction between Fe and Mo oxides, the reduction of Fe was suppressed after the addition of Mo.

K, Ce, and Zr promoters have also been reported to change the catalytic performance of AC-supported Co catalysts.[94] Addition of K to the Co/AC catalyst significantly decreased the FTS activity and CH_4 selectivity. Addition of Ce improved the Co/AC catalyst activity, accompanied by a high CH_4 selectivity. Neither CO_2 nor CH_4 selectivity changed greatly for a Zr-promoted Co/AC catalyst, even though the Zr promoter increased the FTS activity. K, Ce, and Zr promoters improved the Co dispersion and interaction between Co oxide and the AC.

4.1.2. Metal Particle Size Effect, Catalyst Activity and Selectivity. Iron particle size was found to affect the olefin/paraffin (O/P) ratio in FTS. The comparison of small iron particles (1−2 nm) on AC and glassy carbon and larger particles (60−100 nm) on CB showed that the small iron particles in these catalysts exhibited higher O/P ratios (1.2 to 1.8) than a bulk iron catalyst,[82] Fe/Al_2O_3 or Fe/SiO_2 catalysts in FTS.[18] The O/P ratio was found to increase with increasing crystallite size (2.5 to 4.1 nm) for AC- and CB-supported catalysts.[83,85] The decrease in activity with decreasing crystallite size was attributed to structure sensitivity, metal−support interactions in the catalysts, or both.

The olefin/paraffin ratios (O/P) were also affected by catalyst precursors and support sources. Iron catalysts prepared from $Fe(CO)_5$ and the commercial AC showed high O/P ratios.[86,87] CB-, AC-, and glassy-carbon-supported Co or Ru catalysts are highly active and produced mainly paraffins in FTS, which is different from iron/carbon catalysts.[87,89,90]

4.1.3. Microporosity and Deactivation (Sintering and Carbon Deposition). The effect of the porosity of the ACs on the crystallite size and catalytic behavior of Fe/AC catalysts has been studied.[83] The Fe/AC catalyst with the narrowest micropores showed significant blockage of pores. The AC with the widest micropores appears to have prevented metal sintering under both the reduction and the reaction conditions in FTS. Likewise, four ACs (derived from peat, generic wood, pecan, and walnut) containing 75−94% micropores differed considerably in their surface morphology and amounts of micro-, meso-, and macropores.[95] The surfaces of all four ACs were covered primarily by neutral or basic oxygen-containing groups, along with small amounts of acidic oxygen groups (5.6−7.5% oxygen). Metal precursors tended to be present predominantly inside the pores of the peat-, pecan-, and walnut-based ACs, which contained greater amounts of wide pores.

AC-, CB-, and glassy-carbon-supported iron catalysts have been reported to be stable in FTS at 235 °C, whereas Fe/Al_2O_3 catalysts deactivated.[82] In contrast, deactivation was observed on Fe−Mn/carbon catalysts.[96] These catalysts lost approximately ∼50% of their initial activity during the first 24 h, after which they were stable for the next 110 h on-stream. This initial loss is thought to be due to carbon deposition rather than sintering.[96] Likewise, Chen et al. compared the fresh and used catalysts and attributed the deactivation of the carbon supported catalysts to carbon deposition rather than sintering because the catalytic activity could be restored by reduction at 400 °C in H_2.[90] In contrast, other workers were unable to regenerate their carbon-supported catalysts by high-temperature reduction in H_2.[7]

The relation between particle size and sintering for Fe/AC catalysts was studied by Chen et al.[97] They suggested that when there are fewer active sites on the carbon, more of the particles are not bound to the surface, resulting in sintering and deactivation. Thus, small iron particles appear to carburize rather than sinter, and large iron particles, which are less strongly bound to the support, tend to sinter.

DOI: 10.1021/acscatal.5b00090
ACS Catal. 2015, 5, 2640−2658

4.1.4. Summary. Studies done by different researchers on different carbons are difficult to compare because of differences in the support used and the different FT reaction conditions used (H_2/CO ratio, temperature and space velocity). ACs represent a unique class of supports in terms of the kind of metal support interactions obtained. The interaction is generally strong enough to prevent sintering, while not strong enough to inhibit reduction, so that a low-temperature reduction (200 °C) of metal carbonyl clusters is sufficient to activate the catalyst. Several researchers have reduced their catalysts in hydrogen at temperatures that are too high, resulting in gasification of the support. The carbon properties, FTS conditions, and reaction parameters reported in the literature for some CB and AC supported catalyst are summarized in Table 2.

4.2. Catalysts Supported on Carbon Nanofibers (CNFs) and Nanotubes (CNTs). The surface properties of CNTs and CNFs can easily be tailored, and they have hence been considered as model supports in catalysis. To date, the effect of metal particle size,[25,33,42,105−108] pore size,[41,109] pore confinement,[36,38,39,110,111] and promoters[26,35,112−114] on the FTS performances of CNF and CNT-supported catalysts has been extensively studied.

4.2.1. The Effect of Pretreatment and Preparation Methods on the FTS Catalysts. Different pretreatment and catalyst preparation methods affect the surface physical and chemical properties of carbon materials and further affect the performance of catalysts in FTS. The pretreatment methods include purification or functionalization conditions and the use of different calcination conditions.

Several studies have reported the effect of acid treatment on the performance of FTS catalysts. For example, Abbaslou et al.[115] found that acid treatment of CNTs at 25 and 110 °C (35 wt % HNO_3) increased the number of defects and decreased the Fe metal particle sizes for a Fe/CNT catalyst. The Fe/CNT catalyst prepared by pretreatment of CNTs at 110 °C was stable and active, whereas the other acid-treated catalysts experienced rapid deactivation. The Fe/CNT catalyst made on CNTs with a low surface area (25 m^2/g) and larger diameter showed much lower CH_4 and higher C_5^+ selectivities. Likewise, it was found that the surface roughness, together with the degree of surface functionalization of CNTs correlated with the harshness (time and concentration) of the acid treatment.[34] FTS studies on the Fe/CNT catalysts revealed that the more severe the acid treatment of the CNT support, the higher the activity of the catalysts.

Different acid treatments of CNTs were also found to affect the properties of cobalt-based FTS catalysts. In this regard, when CNTs pretreated in 30 wt % HNO_3 were used to prepare Co/CNT catalysts, more defects were formed on the CNT surface.[116] Compared with the fresh Co/CNT catalyst, the cobalt catalysts pretreated in acid showed (Figure 12) (a) increased BET surface area, (b) decreased cobalt particle size and increased cobalt dispersion, (c) increased reducibility, and (d) increased CO conversion. Furthermore, the product selectivity showed a distinct shift to lower molecular weight hydrocarbons after acid treatment.

Different calcination atmospheres (N_2 and air) were found to affect the activity of Co/CNT FTS catalysts.[117] When calcined below 550 °C, the FTS performance was found to be similar for catalysts calcined in N_2 or air. Above 550 °C, the Co/CNT was able to keep its activity because no change in the CNT structure occurred in N_2. The Co/CNT calcined in air lost most of its activity owing to the loss of the CNT structure and sintering of cobalt oxide.

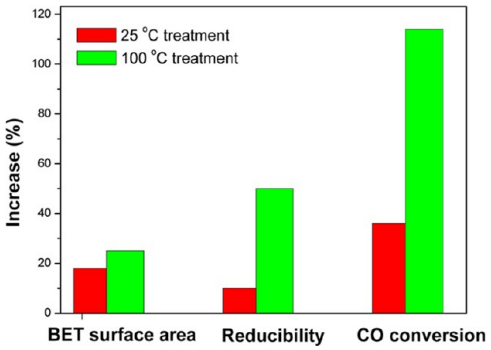

Figure 12. Increase in BET surface area, reducibility and CO conversion for Co/CNT catalysts pretreated using different methods in comparison with a catalyst supported on unmodified CNTs. Data were adapted from ref 34.

Different catalyst preparation methods (impregnation, homogeneous deposition precipitation, and microemulsion techniques) have been investigated for CNF and CNT supported FTS catalysts. For example, it was found that the different preparation methods can significantly affect the FTS performance of the resulting catalysts. Van Steen et al.[118] found that the incipient wetness method and the deposition/precipitation technique using urea yielded highly dispersed Fe^{3+} on the CNTs and the deposition/precipitation technique using K_2CO_3 yielded larger Fe_2O_3 crystallites. The catalyst prepared by incipient wetness was found to be the most active one. The difference in the performance of the catalysts was attributed to the different crystallite sizes.

For Co/CNF catalysts prepared by homogeneous deposition-precipitation (DP) using ammonia evaporation and conventional deposition using urea hydrolysis, the comparison showed that samples prepared at high pH had a 2−4 times higher cobalt-specific activity in FTS than their low-pH counterparts. Likewise, Guczi et al. showed that Co and Fe samples prepared by impregnation were easily reduced.[72] The Fe catalyst prepared by impregnation showed the highest catalytic activity and also a high selectivity toward C_2−C_4 and C_5^+ fractions as well as olefin formation. Catalytic activity was lower for Co and Fe catalysts prepared by the deposition of prepared metal oxide nanoparticles onto a CNT support. Likewise, the comparison of Co/CNT catalysts prepared by microemulsion and incipient wetness impregnation showed that the Co/CNT catalysts synthesized by the microemulsion technique increased the CO conversion by 15% when compared with those prepared by incipient wetness impregnation.[116]

4.2.2. Pore Structure Effects. Catalyst pore structures have been reported to affect the performance of catalysts in FTS.[119−131] This includes both pore size and pore confinement (i.e., particles inside the pore) effects.

Pore Size Effects. For Fe/CNT catalysts, the iron oxide particles prepared on wide pore CNTs (Fe/wp-CNT, 17 nm) were larger than those prepared on narrow pore CNTs (Fe/np-CNT, 11 nm).[36] The extent of reduction of the Fe/np-CNT catalyst was 17% higher when compared with that of the Fe/wp-CNT catalyst. The activity of the Fe/np-CNT catalyst was 2.5 times higher than that of the Fe/wp-CNT catalyst because of the higher degree of reduction and the higher metal dispersion. In addition, the Fe/hp-CNT was more selective toward heavier hydrocarbons compared with that of the Fe/wp-CNT catalyst.

DOI: 10.1021/acscatal.5b00090
ACS Catal. 2015, 5, 2640−2658

The advantages of small-pore CNT supports were also found for Co/CNT catalysts. Lv and co-workers found that by increasing the CNT outer diameter, CO conversion decreased.[117] The data support the conclusion of Xie et al. that a smaller CNT pore size appeared to enhance the Co/CNT catalyst reduction and FTS activity due to the reduced interaction between cobalt oxide with carbon and the enhanced electron shift on the nonplanar carbon tube surface.[109] However, a recent study showed that CNT diameter does not significantly affect the FTS performances of Co/CNTs.[41]

Pore Confinement Effects. Introducing active metals into the support pore can lead to mass transport limitations, which decrease the CO/H_2 ratio inside the pore because of the different diffusion rates of H_2 and CO. Low activity and light hydrocarbon selectivity are observed in FTS products for metal-in-oxide pore catalysts;[121] however, the CNTs showed a completely different pore confinement effect when compared with oxide supports due to the unique electron structure of the convex/concave surfaces of the CNTs.[132]

The effect of pore confinement on FTS has recently attracted extensive attention.[39,109,111,121] Several strategies have been developed to prepare CNT pore-confined catalysts, including in situ filling during surface modification, arc discharge, vapor deposition, and wet chemistry methods.[58,121,133137] Analysis using TEM tilt series experiments (or electron tomography) has been used to distinguish the actual positions of the metal particles on either the external or the internal surface of the CNTs.[73]

The pore confinement effect is closely related to the enhanced autoreduction within the CNT pore. For iron oxide encapsulated within CNTs (Fe-*in*-CNT), Chen et al. reported a reduction temperature that is 200 °C lower than that used to reduce Fe_2O_3 on the outer surface of the CNTs (Fe-*out*-CNT).[110] Furthermore, reduction became easier as the CNT channel diameter decreased.[38] The pore confinement also affected the catalytic reactivity of Fe/CNT catalysts in FTS.[39] The Fe-*in*-CNT was in a more reduced state, tending to form more iron carbides under the reaction conditions. This results in a remarkable modification of the catalytic performance (Figure 13). The yield of C_5^+ hydrocarbons formed over the Fe-*in*-CNT is twice that formed over Fe-*out*-CNT at 30 and 50 bar. Furthermore, diffusion and aggregation of the iron species inside CNTs was retarded as a result of the spatial restriction of the channels. The effect of pore confinement on the reduction, aggregation, and selectivity of Fe/CNT catalyst was confirmed by Abbaslou et al.[112]

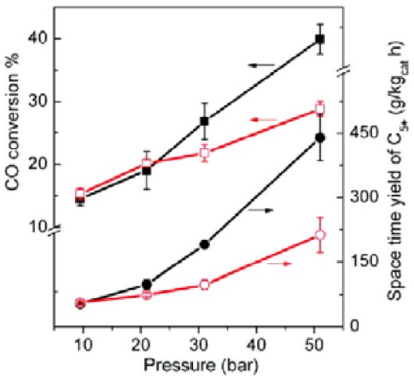

Figure 13. FTS activity of Fe-*in*-CNT and Fe-*out*-CNT at 270 °C as a function of pressure. Square symbols represent CO conversion; circles, the space−time yield of C_5^+ hydrocarbons. Filled symbols denote Fe-*in*-CNT; open ones denote Fe-*out*-CNT. Reprinted with permission from ref 39 (Chen, W.; Fan, Z.; Pan, X.; Bao, X. *J. Am. Chem. Soc.* **2008**, *130*, 9414−9419); copyright 2014, American Chemical Society.

The enhanced reduction effect of pore confinement was also found for Co/CNT catalysts, with Co particles inside CNTs being easier to reduce than Co particles placed outside the CNT.[109] The activity of the catalyst with Co inside a CNT was higher than that of catalysts with Co particles outside a CNT; however, a recent study showed that for CNTs, with pore sizes of 5−20 nm, the C_5^+ hydrocarbon selectivity showed no difference between cobalt particles confined in a CNT pore (Co/CNT-in) and for cobalt outside the CNT pore (Co/CNT-out), even though the pore-confined Co/CNT-in catalyst was found to reduce more easily in comparison to the Co/CNT-out catalyst.[33] These data suggest that the pore-confinement effect for CNTs is essentially related to the effect of the interaction that results from the different surface electronic properties of CNTs inside and outside the tubes.

4.2.3. Metal Particle Size Effects. As mentioned, CNFs and CNTs have been studied as model catalyst supports to investigate the role of the metal particle size on FTS as it relates to the metal−carbon interaction.[25,27,105−107,113,138,139] De Jong's group systematically investigated the metal particle size effect for both Fe/CNF and Co/CNF catalysts.[25,139] They found that the surface-specific activity (apparent TOF) of unpromoted Fe/CNF catalysts increased 6−8-fold when the average iron carbide size decreased from 7 to 2 nm, while methane and lower olefin selectivities were not affected.[139] The turnover frequency (TOF) was independent of cobalt particle size for catalysts with sizes larger than 6 nm (1 bar) or 8 nm (35 bar), and both the selectivity and the activity changed for catalysts with smaller particle sizes (Figure 14).[25] For small Co particles (<6 nm), the surface residence times of reversibly bonded CH_x and OH_x intermediates increased, whereas that of CO decreased.[105] A higher coverage of irreversibly bonded CO was found for small Co particles that were ascribed to a larger fraction of low-coordination surface sites. The higher methane selectivity of small Co particles is mainly due to their higher hydrogen coverage.

A comparison of the surface similarity of CNTs and carbon spheres (CSs) has revealed that the TOF value for both Co/CNTs and Co/CSs was constant for cobalt particles above 10 nm and decreased sharply for the cobalt catalysts with smaller cobalt particles.[33] Thus, the TOF for cobalt catalysts on two different carbon supports depends only on particle size.

Structure sensitivity was also found on Ru/CNT FTS catalysts.[42] Both the C_{10}-C_{20} hydrocarbon selectivity and the TOF for CO conversion was found to depend on the mean size of the Ru particles, and a Ru/CNT catalyst with a mean Ru size of approximately 7 nm exhibited the best C_{10}−C_{20} selectivity and a relatively higher TOF.

4.2.4. Reduction and Promoter Effects. CNF- and CNT-supported catalysts have been shown to exhibit a weak metal−support interaction and a high extent of reduction.[41] Several promoters have been added to these catalysts to modify the FTS performance, especially the product selectivity. Promoters for iron catalysts are typically Mo, K, Cu, and Mn, whereas noble metals such as Pt and Ru are usually added to Co/CNT and Co/CNF catalysts.

A comparison of unpromoted Fe/CNT and catalysts promoted with different Mo contents (0.5, 1, 5, and 12 wt %) indicated that the addition of Mo resulted in the formation of smaller Fe particles and an increased Fe reduction temperature

DOI: 10.1021/acscatal.5b00090
ACS Catal. 2015, 5, 2640−2658

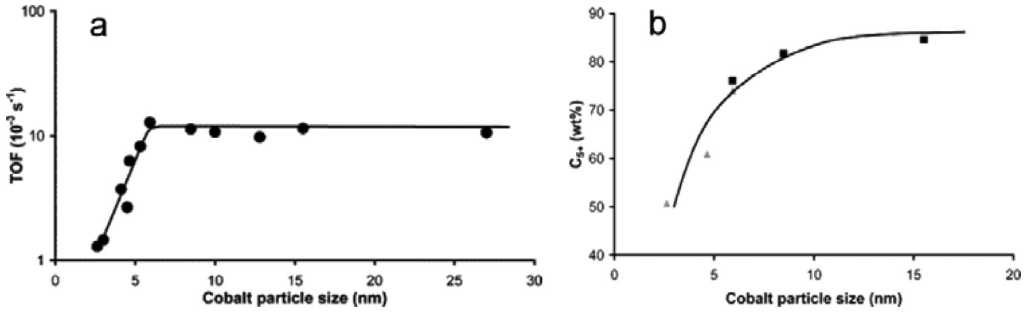

Figure 14. Influence of cobalt particle size on (a) the TOF (220 °C, H_2/CO = 2, 1 bar) and (b) the C_5^+ selectivity measured at 35 bar; data markers in black at 210 °C and in gray at 250 °C. Reprinted from ref 25 (Bezemer, G. L.; Bitter, J. H.; Kuipers, H. P. C. E.; Oosterbeek, H.; Holewijn, J. E.; Xu, X.; Kapteijn, F.; van Dillen, A. J.; de Jong, K. P. *J. Am. Chem. Soc.* **2006**, *128*, 3956−3964); copyright 2014, American Chemical Society.

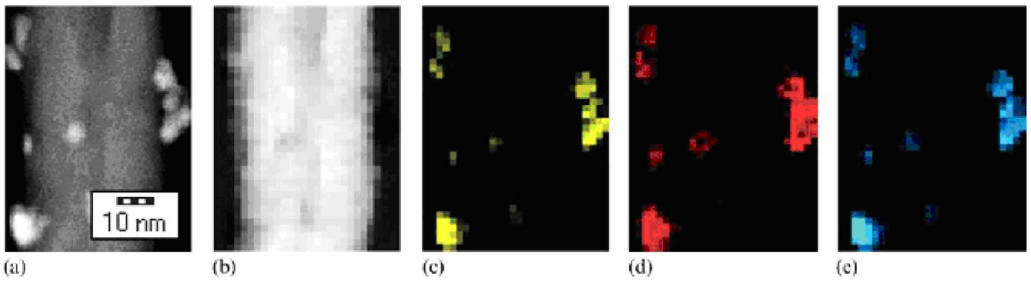

Figure 15. Representative images of dried CoMn/CNF: (a) HAADF image and elemental mappings for (b) carbon, (c) cobalt, (d) manganese and (e) oxygen. Reproduced from ref 26 with permission from The Royal Society of Chemistry.

due to the decreased particle size of the iron oxides.[140] Moreover, the addition of 0.5−1 wt % Mo resulted in a more stable catalyst, whereas higher contents of Mo (5 and 12 wt %) decreased the activity of the catalysts as a result of catalytic site coverage and a lower extent of reduction. However, Mo promotion (0.5−12 wt %) increased the selectivity of the catalysts toward lighter hydrocarbons.

K-promoted Fe/CNT catalysts gave suppressed reduction, decreased FT rate, higher yields of CO_2, and a lower methane selectivity when compared with unpromoted catalysts.[114,141] The addition of copper did not have an effect on the FT product selectivity, but it enhanced catalyst activity. Likewise, for a bimetallic Fe−Ru/CNT catalyst, the effect of the promoters K and Cu on the small bimetallic particles (2.1 nm) followed trends similar to what was observed on promoted Fe/CNT catalysts.[37] This suggests that metal−support interactions do not strongly affect the promoter properties of the metals.

Promotion with Mn suppressed both hydrogen chemisorption and cobalt reducibility.[113] At 1 bar, large improvements in the selectivity toward C_5^+ products were found with MnO loadings of ≥0.3 wt %. At 20 bar, the addition of only 0.03 wt % MnO improved the C_5^+ selectivity, but the C_5^+ selectivity decreased to 52 wt % with 1.1 wt % MnO. The surface-specific activity (TOF) first increased with a MnO loading of 0.3 wt %, whereas it decreased at MnO loadings >0.3 wt %. STEM-EDX mapping showed that MnO is associated with Co in both the dried and reduced catalyst (Figure 15).

The addition of promoters Pt and Ru to a Co/CNT catalyst significantly decreased the reduction temperature of the cobalt species, but it had no significant effect on the cobalt particle size.[35] Promotion of Co/CNT catalysts with small amounts of Pt and Ru resulted in a slight increase in FT cobalt time yield. The Pt-promoted Co/CNT was more stable than the unpromoted cobalt catalyst. Trépanier and co-workers found that Ru enhanced the reducibility of Co_3O_4 to CoO and that of CoO to Co^0 for Co/CNT catalysts, and this increased the FTS rate and enhanced the selectivity of FTS toward the higher molecular weight hydrocarbons.[114] The Pt increased the dispersion and decreased the average cobalt cluster size.

4.2.5. Stability of FTS Catalysts Supported on CNFs and CNTs. Fe/CNT catalysts have been reported to deactivate with time on stream.[118] However, in a subsequent study, both unpromoted Fe/CNT and the promoted catalysts with K or Cu showed very stable activity.[141] Likewise, bimetallic Fe−Ru/CNT catalysts also showed stable activity in the FT reaction (∼120 h).[37] Abbaslou and co-workers reported that Fe/CNTs pretreated at 110 °C in $HNO_{3(aq)}$ gave a very stable and active catalyst during 120 h FTS on stream, but iron catalysts supported on pristine CNTs and CNTs treated under mildly acidic conditions deactivated within the same reaction period.[115] Detailed microscopy characterization results revealed that the mobility of surface-bound metallic nanoparticles (NPs) on catalyst supports resulted in agglomeration, leading to a consequent decrease in the catalytic activity of the metal NPs over time.[142] The enhanced effect of "docking stations" along the exterior of the CNT can limit the surface mobility of ultrasmall iron particles on CNT surfaces during FTS.

A recent study has investigated the effects of the electronic properties of the inner and outer surfaces of CNTs on the deactivation of Co/CNT catalysts during FTS.[111] The comparative characterization of the fresh and used Co/CNT catalysts showed that cobalt reoxidation, cobalt−support interactions, and sintering are the main sources of catalyst deactivation. In contrast, using in situ Mössbauer spectroscopy, oxidation of the Co nanoparticles for a Co/CNF catalyst by water was shown not to occur when H_2 is present.[143] Only in a H_2O/Ar atmosphere did oxidation take place. At a relative humidity (RH) below 25%, sintering was absent, even after 4 weeks of reaction, whereas at a high RH of 62%, as much as half of the small superparamagnetic cobalt particles (<5 nm) sintered

DOI: 10.1021/acscatal.5b00090
ACS Catal. 2015, 5, 2640−2658

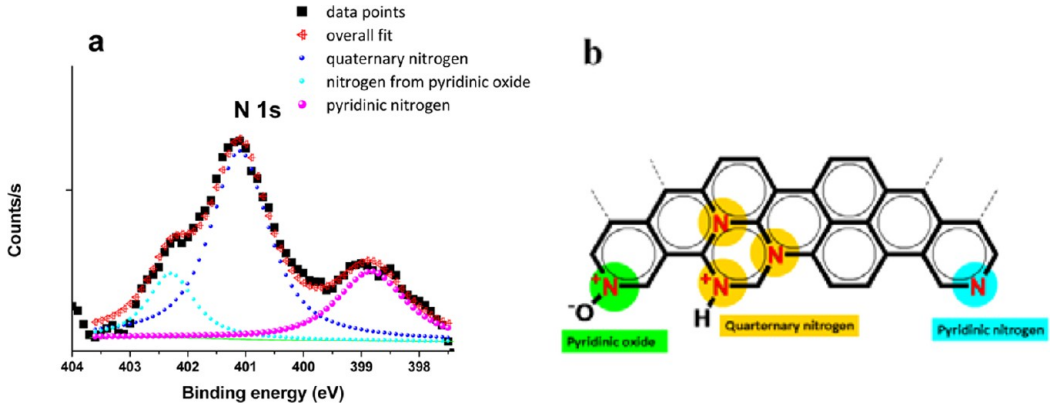

Figure 16. N 1s XPS spectra of (a) N-CNT and (b) figure showing the types of nitrogen species on the nitrogen-doped carbon nanotubes prepared by postdoping method. Reprinted from ref 78 (Xiong, H.; Motchelaho, M. A.;Moyo, M.; Jewell, L. L.; Coville, N. J. Fischer−Tropsch synthesis: Iron-based catalysts supported on nitrogen-doped carbon nanotubes synthesized by postdoping. *Appl. Catal., A* **2014**, *482*, 377−386); copyright 2014, with permission from Elsevier.

into larger particles in 1 week. The cobalt particles in the inner tube of the CNF material sintered to a lesser extent (up to 8 nm), which revealed the benefit of tube confinement against sintering.

4.3. Catalysts Supported on Ordered Mesoporous Carbon (OMC). Ordered mesoporous carbons (OMCs) have a 3D pore structure, which enhances the transport of reactants and products to and from catalytic metal sites on the OMCs.[144,145] The OMCs have advantages as supports in that (i) the pores are large and diffusion issues are not important, (ii) impregnation of metals is influenced by carbon acid pretreatment, and (iii) the OMC structure inhibits metal catalyst sintering. Because OMCs are made with templates, template removal is an issue of importance in their use.[57,146] In addition, it is still difficult to achieve uniformly dispersed crystalline nanoparticles at high concentrations in the mesopores of a carbon support.[147]

To date, not many studies have been performed on FT catalysts supported on OMCs. Fu et al. have reported a study in which cobalt catalysts supported on an ordered mesoporous carbon (CMK-3) was used in FTS.[148] It was found that Co_3O_4 particles were mainly dispersed inside the pores of the Co/CMK-3.

Ru catalysts supported on OMC have recently been investigated in FTS.[149,150] The catalysts were synthesized by either an autoreduction reaction (Ru-OMC) or impregnation (Ru/OMC) process.[149] Both Ru OMC catalysts exhibited a highly ordered mesoporous structure and a large surface area. The Ru particles on Ru-OMC were found to be embedded in the OMC wall. Compared with Ru/OMC, Ru nanoparticles on Ru-OMC were in intimate contact with the carbon supports and had a superior activity. This feature may create certain electron-deficient sheets upon interfacial contact, which facilitates the transfer of spilled-over hydrogen and improves hydrogen dissociation on the catalyst surface.

4.4. Catalysts Supported on Graphene, Graphite, Diamond and Carbon Spheres. *Graphene.* Small and stable Fe_2O_3 nanoparticles have been homogeneously anchored onto reduced graphene oxide through the simultaneous hydrolysis of $Fe(acac)_3$ and the reduction of graphene oxide.[151] This nanohybrid is highly resistant to sintering and retains its small particle size upon reduction at 450 °C and is stable in the long term for FTS at 270 °C.

Diamond. The FTS behavior of a Co-loaded oxidized diamond (O−Dia) catalyst having a surface area of 24 m^2/g has been reported by Honsho et al.[152] The Co/oxidized diamond catalyst exhibited a high CO conversion of 44.5%. This conversion was much higher than that of two Co/SiO_2 catalysts with surface areas of 190 and 12 m^2/g.

Carbon Spheres (CSs). Because of their inert surface and nonporous nature when prepared by CVD procedures, CSs have been regarded as model catalyst supports to investigate the effect of different reaction parameters (metal particle size, promoters, and deactivation) in FTS.[55,153,154] An investigation of the effect of the preparation method, iron precursor, and promoters on Fe/CS catalyst showed a good match of FT activity and selectivity results when the data were compared with studies on noncarbon supports. Furthermore, Co oxides can be autoreduced by the carbon spheres. The autoreduced catalyst showed a better FTS performance in comparison with a catalyst reduced in H_2.[33,153]

A CS-supported Fe catalyst prepared by a hydrothermal method has been tested in FTS.[155] The iron oxide nanoparticles were found to embed in the CSs and were highly dispersed in the carbonaceous spheres, leading to a unique microstructure. The reduced catalyst showed a remarkable stability and selectivity in FTS.

Carbon spheres prepared using the hydrothermal method were also used to support cobalt catalysts for FTS.[156] Catalysts were prepared by an evaporative method (Co/CS-IWI) and by a chemical vapor deposition technique (Co/CS-CVD). The CVD technique led to a higher CO conversion (26.5%) relative to the conventional evaporative (IWI) method (7.4%). The difference in the CO conversion between Co/CS-IWI and Co/CS-CVD catalysts was due to the smaller average Co particle size and more uniform distribution resulting from the CVD method.

4.5. Catalysts Supported on Heteroatom-Doped Carbon Materials. Raw carbon materials must be treated in acid or oxidized to produce functional groups on the carbon surface to efficiently anchor metal or metal oxide species on the carbon. The use of heteroatom-doped carbon materials as supports can avoid this step because the heteroatom can act as an anchoring site. These heteroatom-doped carbon materials have been used as catalyst supports in FTS.[78,157,158]

For example, iron nanoparticles have been loaded onto N-CNTs without surface premodification.[43] The Fe/N-CNT catalyst had superb catalytic performance in FTS, with high selectivity for lower olefins (up to 46.7%) as well as high activity and stability. The performance was well-correlated with enhanced dissociative adsorption of CO, inhibition of secondary hydrogenation of lower olefins, and promotion of the formation

DOI: 10.1021/acscatal.5b00090
ACS Catal. 2015, 5, 2640−2658

of the active phase of χ-Fe_5C_2. All of these advantages have been attributed to the participation of the nitrogen atoms. Likewise, an approach has been recently developed to prepare N-CNTs by a postdoping method (onto CNTs) at 700−900 °C.[78] The nitrogen atoms were found to homogeneously disperse on the CNT surface (so that the resulting N-CNTs contained 1.75% nitrogen). The N was in the form of pyridinic N atoms, quaternary N atoms, and N atoms from pyridinic oxide (Figure 16). Because of the incorporation of nitrogen atoms, the Fe/N-CNT catalyst was harder to reduce than the corresponding Fe/CNT catalyst. The interactions between iron oxides and carbon supports significantly affected the FTS performance: the Fe/N-CNT catalysts had superior FTS activity when compared with Fe/CNT catalysts.

Nitrogen-doped carbon spheres were also used to load iron particles without a functionalization step.[158] The FTS performance of three Fe/NCS catalysts was found to correlate with the Fe particle size, which was influenced by the N content, the N type, and the defect sites. It was suggested that pyrollic and pyridinic N atoms played a key role in binding the Fe atoms and that quaternary N atoms played a minor role. The Fe/NCS_{ver} (NCSs prepared in a vertical tube furnace) contained well-dispersed Fe oxide particles on CSs that had the highest N content (made of pyrollic/pyridinic N atoms), and this led to the highest FT activity. The Fe/NCS_{hor} catalyst (NCSs prepared in a horizontal tube furnace) showed the lowest FT activity as a result of the presence of the largest Fe oxide particles (50% quaternary N atoms).

Likewise, for nitrogen-doped ordered mesoporous carbon (OMC)-supported cobalt particles, the doped nitrogen atoms, especially the pyridine-like nitrogen, served as the anchoring sites for cobalt species.[159] Furthermore, a more uniform cobalt particle size was observed for the catalysts supported on nitrogen-doped OMC in comparison with the catalysts supported on pristine OMC. In contrast, the autoreduction temperature of cobalt oxide in the catalysts was considerably lower after nitrogen doping, and the cobalt specific activity on the nitrogen-doped OMC was 1.5 times higher than its analogue on the pristine OMC.

The origin of the role of the nitrogen embedded in the carbon matrix on the activity of the supported metal has been extensively studied. It has been proposed that an electronic modification of a metal occurs when a metal interacts with a carbon surface via a π−d (carbon−metal) interaction.[160] The presence of the N further distorts this interaction, hence leading to modified metal−carbon interactions. However, N also introduces more defects into a structure (at edges/in the carbon plane etc.), and this could also impact the carbon−metal interaction.

4.6. Catalysts Supported on Hierarchical Carbons. The FT reaction is exothermic, and this can lead to hotspots and thermal runaway if the heat of the reaction is not dissipated. In the past, this was achieved via reactor design or reactor choice. An alternative is to remove the heat generated via the support. In the past, FT supports were typically metal oxides (Al_2O_3, SiO_2, TiO_2, etc.), and thus, insulators. Carbons, by contrast, are thermally conductive.[161,162] The thermal conductivity of CNTs is ∼3000 W/m-K (compare with diamond, between 900 and 2300 W/m-K, and copper at 400 W/m-K).[163] Not only are they conductive, but their lack of microporosity has aided in alleviating the thermal dissipation issue. However, because the carbons are nanosized, there are still problems associated with pressure drop in a reactor when carbons are to be used as supports. The carbons are also prone to oxidation, a reaction catalyzed by the FT catalyst, and this can also lead to hotspots. To overcome these issues, a number of alternative approaches have been used, including the generation of hierarchical structures (see below) and the use of alternative supports, such as SiC.[164]

Important characteristics of an industrial catalyst are the chemical composition, surface area, stability, and mechanical properties. Furthermore, for an industrial FT reaction carried out in a packed bed reactor, the catalyst requires an appropriate diameter to achieve a tolerable pressure drop. Thus, attempts have been made to grow/attach CNTs onto a secondary support to overcome this problem. A simple approach has been to grow CNTs onto a carbon nanofiber (CNF) or CNFs onto a carbon felt to maintain an all-carbon support.[165,166] A compact, fixed-bed reactor made of disks of the composite material showed improved heat and mass transfer, a relatively low pressure drop, and safe handling of the immobilized CNFs. An efficient 3-D thermal conductive network in the composite provided a relatively uniform temperature profile, and the open structure of the CNF-felt composites afforded very good accessibility to the Co nanoparticles during FT synthesis in the fixed bed reactor.

Hierarchical structures in which carbons have been grown/attached to metal oxides has also been explored. A hierarchical composite consisting of a CNT layer anchored on a macroscopic α-Al_2O_3 host matrix has been developed as a support for this purpose in FTS.[167] The composite, consisting of a thin shell of a homogeneous, highly entangled and structure-opened CNT network, exhibited a relatively high and fully accessible specific surface area of 76 $m^2 \cdot g^{-1}$, compared with a surface area of 5 $m^2 \cdot g^{-1}$ for the original α-Al_2O_3 support. This hierarchically supported cobalt catalyst exhibited a high FTS activity along with a high selectivity toward liquid hydrocarbons compared with a cobalt-based catalyst supported on pristine α-Al_2O_3 or on CNTs. This improvement can be attributed to improved mass transfer for the composite surface compared with the macroscopic host structure (pore diffusion) or the CNTs alone (film mass transfer). Cobalt supported on the CNT decorated α-Al_2O_3 catalyst was also stable over more than 200 h on-stream under relatively severe conditions. Finally, the macroscopic shape of such composites allowed its use as a catalyst support in a fixed-bed configuration without the problems of transport and pressure drop as encountered with CNTs. Recently, the FT activity and C_5^+ selectivity of a hierarchical Co/CNT-Al_2O_3 catalyst was found to be further improved by adding TiO_2 nanoparticles into the catalyst.[8] The addition of TiO_2 (added as $Ti(O^iPr)_4$) affected the support surface area, pore volume, Co particle size, etc., but importantly, the macroporosity was enhanced, and this led to good catalyst stability and a good C_5^+ selectivity of >85%.

There is a further issue that relates to making fuels via FTS and HAS routes—the possibility of converting the primary FTS (or HAS) products using a second catalyst into upgraded fuels in the same reactor. In this instance, the second catalyst requires an acidic function to bring about isomerization reactions. This area of FTS study has been investigated with the more classical oxide supports for decades, and more recently, some studies have been reported using carbon supports.[12] Results to date have been modest.

4.7. Comparison of Catalysts Supported on Shaped Carbons and Metal Oxides. A recent study revealed that Fe/CNF is an excellent catalyst system for the conversion of synthesis gas to C_2−C_4 olefins with selectivity up to 60 wt % compared with oxide-supported catalysts.[168] Likewise, the comparison of Co catalysts supported on CNFs, α-Al_2O_3 and

DOI: 10.1021/acscatal.5b00090
ACS Catal. 2015, 5, 2640−2658

γ-Al_2O_3, showed that the CNF-supported catalyst has a high activity and high selectivity to C_5^+ hydrocarbons in FTS when compared with Co/γ-Al_2O_3 and Co/α-Al_2O_3.[169] The activity was directly correlated to the dispersion of the cobalt particles on carbon-supported catalysts. Possible explanations for the high selectivity to C_5^+ hydrocarbons for carbon-supported catalysts are that the CNFs are free of micropores and exert less transport limitations for the reactants and products or that the adsorption ratio of CO/H_2 is always higher on carbon-supported cobalt catalysts than on alumina-supported cobalt.

In another study, Co catalysts supported on unpurified CNTs grown on MgO and Al_2O_3 were compared with activated carbon as well as Al_2O_3 in FTS.[170] The results revealed that the activity of the Co/CNT catalyst improved as a result of a higher degree of reduction, as compared with the Co/Al_2O_3 catalyst. In addition, the Co/CNTs grown on MgO (Co/CNT−MgO) showed the highest C_5^+ selectivity and olefin/paraffin ratio, which were ascribed to a synergetic effect between the CNTs and MgO.

A comparative study of cobalt catalysts supported on CNTs, CNFs and CMCs in FTS revealed that the different supports affected the appearance, size, and dispersion of cobalt particles as well as their reducibility (Figure 17).[45] The Co reducibility and

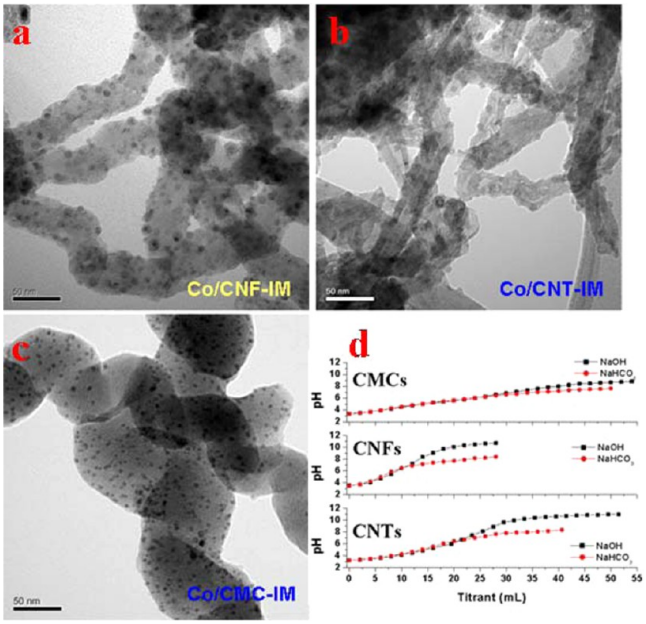

Figure 17. TEM images of (a) Co/CNFs, (b) Co/CNTs, (c) Co/CMCs, and (d) the titration curves of CMCs, CNFs, and CNTs. Reprinted from ref 45 (Xiong, H.; Motchelaho, M. A. M.; Moyo, M.; Jewell, L. L.; Coville, N. J. Cobalt catalysts supported on a microcoil carbon in Fischer−Tropsch synthesis: A comparison with CNTs and CNFs. *Catal. Today* **2013**, *214*, 50−60); copyright 2014, with permission from Elsevier.

dispersion on the differently shaped carbon supports was influenced (and tuned) by modifying the functionalization on the support surface, that is, by changing the metal−support interactions.

A study that compared cobalt catalysts supported on ordered mesoporous carbon (CMK-3), CNTs and AC showed that Co_3O_4 particles were dispersed mainly inside the pores of the Co/CNTs and Co/CMK-3 but outside the pores of Co/AC.[148] Cobalt particles on Co/CNT maintained their original size because of their confinement in the central pore of the CNTs, but the ordered structure of CMK-3 was partially destroyed in the process of catalyst preparation. CNTs were more stable at high temperature in an H_2 atmosphere than either CMK-3 or AC, and the reduction degree of Co/CNTs was found to be higher than the other two catalysts. The Co/CNT showed a better performance for FTS than the Co/CMK-3 and Co/AC catalysts.

5. SHAPED CARBONS USED AS SUPPORTS FOR THE CONVERSION OF SYNGAS TO ALCOHOLS

An alternative to converting syngas to hydrocarbons is to convert syngas to alcohols. These alcohols can then be used in fuels (directly) or as an additive to hydrocarbon fuels. As with FTS, most catalysts used for the conversion process are supported catalysts, and the supported catalysts showed high activity and selectivity for alcohols in higher alcohols synthesis (HAS) from syngas. These supports include shaped carbon materials.[171] As shown in Table 3, the metals Mo, Rh, Cu, and Co have all been shown to be active components, and the metal ions Mn and K are promoters in this reaction. In particular, shaped carbon-supported Mo and Rh catalysts have been extensively studied because they have shown high activity and selectivity for HAS from syngas.

5.1. Activated Carbon (AC)-Supported Catalysts.

5.1.1. Active Phase, Reduction and Promoters. Cu/AC catalysts have been studied in HAS from syngas.[172] It has been shown that metallic copper is the active phase in the reaction. In contrast, the active sites are Co and Co_2C for a Co−Zr−La/AC catalyst.[173] The total alcohol selectivity was in the range of 40.5−62.3%, and the selectivity for C_6^+ alcohols was between 12.6 and 40.3%.

Analysis of Mo/AC catalysts revealed a new phase related to the interaction between Mo species and the AC support.[174] Mo species with intermediate valence values (on average, around +3.5) were likely to be the active phase(s) for HAS from syngas. In contrast, for AC-supported K_2CO_3/Co-MoS_2 catalysts, the active ingredients were molysulfide and cobalt sulfide.[175] The main active phases for AC-supported Mo catalysts are dependent on the catalyst composition and whether they are oxidic or sulfided Mo-based catalysts.[200] In the oxidized state, the Mo on a Mo−K/AC sample with low Mo loading is mainly present as MoO_2. As the Mo loading increases, the interaction between K and Mo is enhanced. Mo exists mainly in the form of K−Mo−O species. After sulfidation, the Mo sulfide phase was highly dispersed as tiny three-dimensional particles at high loading, and MoS_2 was the major phase present in Mo−K/AC.

The addition of a K promoter was observed to increase the higher alcohol selectivity.[171,176] This is because the addition of K greatly promotes the formation of Mo species, which are reducible at relatively low temperatures, while it retards the generation of Mo species that are reducible only at high temperatures.[174]

Other promoters, such as Rh, Co, Ni, Cr, and Cl, have also been found to affect the performance of AC-supported MoS_2 catalysts in HAS from syngas.[177,201] The addition of Rh resulted in an enhanced dispersion of smaller-sized Mo particles. The addition of promoters (Ni, Co and Rh) improved the reducibility of the catalyst and shifted the reduction of Mo^{6+} to lower temperature. Furthermore, Ni−Mo−S and Co−Mo−S phases were formed in the Ni- and Co-promoted MoS_2 catalysts. The addition of Co, Cr and Cl to K−Mo/AC led to an increase in either the alcohol activity or selectivity.

5.1.2. The Effect of Preparation Procedures and Activated Carbon Texture. The effects of catalyst preparation parameters

DOI: 10.1021/acscatal.5b00090
ACS Catal. 2015, 5, 2640−2658

Table 3. Catalyst Composition, Reaction Conditions and Alcohols Selectivity in HAS from Syngas over Shaped Carbon-Materials-Supported Catalysts[a]

shaped carbon materials	catalyst	reaction conditions	alcohol selectivity	reference
activated carbon	Cu/AC	30 bar, 300 °C	75%	172
	Co−Zr−La/AC	30 bar, 220 °C	40.5−62.3%	173
	Mo−K/AC	5.1 MPa, 200−400 °C	N.A.	174
	K_2CO_3/CoS/MoS_2/AC	13.8−16.5 MPa, 270−330 °C	79−89%	175
	MoC_2−K/AC	100 bar, 260−280 °C	1.6−70.2%	171
	Mo−K−Co/AC	0−1500 psi, 200−400 °C	N.A.	176
	Co-, Ni-, Rh-MoS_2−K/AC	8.3 MPa, 320 °C	21−49%	177
	Co−K−Zr/AC	3.0 MPa, 222 °C	9.6−60.9%	178
	Co−Rh−MoS_2/AC	8.3 MPa, 330 °C	24−28%	179
carbon nanotubes	Mn−Rh/CNT	2.0−5.0 MPa, 280−320 °C	23.8−31.9%	180
	Co−Cu/CNT	5.0 MPa, 250−310 °C	50−70%	181, 182
	$Ni_1Mo_1K_{0.05}$/CNT	5.0 MPa, 265 °C	59.0%	183
	Ni−K−MoS_2/CNT	8.0 MPa, 320 °C	33.1−64.1%	184
	Co−K−MoS_2/CNT	2.0−5.0 MPa, 300−350 °C	40−70%	185
	Mo−K/CNT, K-MoS_2/CNT	70 bar, 320 °C	45.3−65.2%	186, 187
	K−Co−Rh-MoS_2/CNT	800−1400 psi, 270−350 °C	35.6%	179, 188
	Cu−Co/CNT	4.0 MPa, 290 °C	69%	189
	MoS_2−Co−Rh-K/CNT	8.3 MPa, 330 °C	28.7−85.7%	190
	Co-, Ni-doped Mo−K/CNT	2.0−8.0 MPa, 215−330 °C	19.5−85%	191−193
	Rh−Mo−K/CNT	5.51−9.65 MPa, 300−340 °C	17.8−33.2%	194
	Co−K−MoS_2/CNT	5.51−9.65 MPa, 300−340 °C	20.3−34.1%	195
	Mn/Rh/CNT	20 bar, 290 °C	20−60%	40
	Rh−Mn−Li-Fe/CNT	3.0 MPa, 320 °C	38−64.6%	196
mesoporous carbon	MoC_2/OMC	3.0 MPa, 300 °C	56.1−84.1%	197
	Rh/OMC	3.0 MPa, 320 °C	32.4−56.4%	198, 199

[a]N.A. = not available.

(Mo precursor, Mo loading, and pretreatment) and the reaction conditions (temperature and space velocity) on Mo−K/AC catalysts have been studied for the HAS from syngas.[176,201,202] The Mo loading was found to influence the reducibility of the K−Mo/AC catalysts.[202] An increase in reaction temperature gave a monotonic decrease in the selectivity toward alcohols, and a maximum in the space time yield (STY) of alcohols. Increasing the space velocity increased the STY and selectivity to alcohols. Likewise, for K_2CO_3/Co-MoS_2/AC catalysts, total alcohol productivity also increased with an increase in space velocity.[175]

The AC characteristics were found to affect the performances of AC-supported catalysts in HAS from syngas. For example, for sulfided Co−Rh−Mo catalysts supported on microporous and mesoporous ACs, the formation of large particles took place as a result of the agglomeration of metal species on the microporous AC.[179] For Co catalysts supported on two ACs with similar porous texture, the selectivity for C_1−C_{18} alcohols over Co/AC1 (the AC was made from coconut shell) and Co/AC2 (the AC was made from almond shell) were 20.6% and 9.6%, respectively.[178] This difference in alcohol selectivity arose from the different types and amounts of surface oxygen-containing groups on the ACs, which influenced the Co phases and led to different performances for the catalysts. Likewise, for a Co−Zr−La/AC catalyst, nitric acid pretreatment led to a significant increase in surface oxygen groups on the AC.[173]

5.2. Carbon Nanotube (CNT)-Supported Catalysts. *5.2.1. The Effect of Preparation Parameters and Reaction Conditions.* Similar to the behavior of the pretreated AC supported catalysts, HNO_3-pretreatment of CNTs was found to promote the performance of CNT-supported catalysts in HAS from syngas.[189] The CO conversion and alcohol yield of an HNO_3-pretreated Cu−Co/CNT catalyst increased by ∼21% and 69%, respectively, compared with those for the unpretreated Cu−Co/CNT catalyst.

The catalyst preparation method affected the activity and selectivity of CNT-supported Mo catalysts in HAS from syngas. In this regard, CNT-supported MoS_2−K catalysts prepared using impregnation and microemulsion techniques have been compared.[187] A narrow particle size distribution was produced by the microemulsion technique, and the dispersion increased to 60.8% and the reduction increased by 43%. The CNT-supported MoO_3−K_2O catalyst synthesized by the microemulsion technique increased the alcohol selectivity to 65.2%.

The effects of operating conditions on the HAS were studied using a CNT-supported sulfided K−Co−Rh−Mo catalyst.[188] The CO conversion increased monotonically with increasing reaction temperature and pressure, and it decreased monotonically with increasing space velocity. Likewise, for a Mn-promoted Rh/CNT catalyst, an increase in pressure gave an increase in alcohol selectivity.[180] Finally, the presence of CO_2 in the feed syngas over a CNT-supported catalyst was beneficial to CO conversion and the selective formation of alcohols.[181,182]

5.2.2. The Effect of Promoters on the Catalyst Performances. Similar to the behavior of AC-supported Mo catalysts, the addition of K into a Mo/CNT catalyst improved the alcohol selectivity.[171,186] The increased selectivity to higher alcohols (45.3 wt %) was due to the presence of the K−Mo−O phases. An enhancement of the formation of higher alcohols by K−Mo−O phases was also found for Co- and Rh-promoted Mo−K/CNT catalysts.[194,195,203]

CNT-promoted Co−Cu and Ni−Mo−K catalysts displayed excellent performance for the selective formation of C_{2-4} oxygenates from syngas.[181−185,204] The mass percent of BuOH and DME reached 83%. The addition of a minor amount of the

DOI: 10.1021/acscatal.5b00090
ACS Catal. 2015, 5, 2640−2658

CNTs to the hosts led to an increase in the surface concentration of catalytically active CoO(OH), NiO(OH), and Mo^{4+}/Mo^{5+}, which are closely related to the selective formation of higher alcohols. The promotion of alcohols and surface species was also found for the Ni- or Co-decorated CNT-promoted Ni−Mo−K or Co−Mo−K catalysts.[191−193] The enhanced alcohol selectivity was ascribed to the CNTs that provided the sp^2-C surface sites for adsorption−activation of H_2.

A study of Mn promotion on the performance of Rh/CNTs revealed that after the addition of Mn, CO conversion and ethanol yield increased significantly in HAS from syngas.[40,180] The high activity of the Mn−Rh/CNT catalyst and the corresponding high ethanol yield were attributed to the small active components. Because of the presence of CNTs, the Mn−Rh interactions were observed at atomic resolution during STEM-EELS, and ∼1 nm Rh particles were found in the promoted and unpromoted catalysts. The STEM and EELS results verified the enhanced metal−promoter interaction when the amount of Mn promoter increased from 1 to 2 wt % (Figure 18). The enhancement in the degree of metal-promoter interaction led to an increase in the ethanol selectivity.

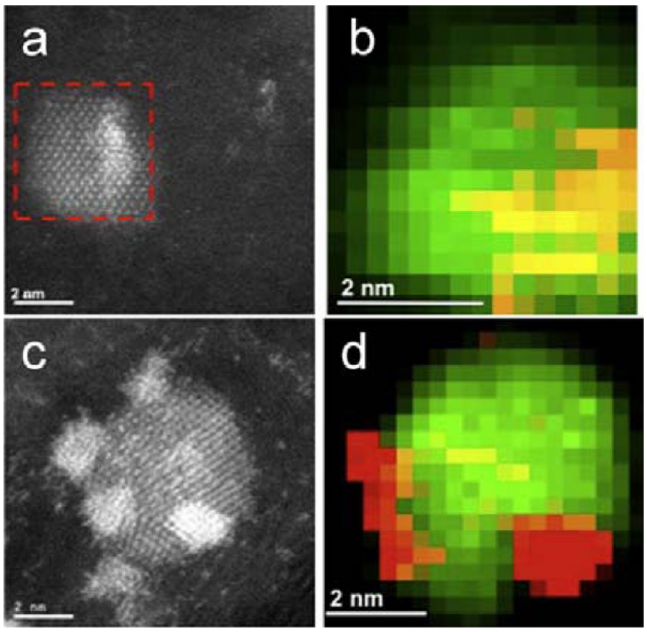

Figure 18. High-resolution STEM imaging and the EELS mapping of representative areas on (a, b) 1% Mn−3% Rh/CNT and (c, d) 2% Mn−3% Rh/CNT catalysts. The Rh signal is shown in red, and the Mn signal is shown in green. The orange and yellow are caused by the overlap of Rh and Mn. Reprinted from ref 40 (Liu, J. J.; Guo, Z.; Childers, D.; Schweitzer, N.; Marshall, C. L.; Klie, R. F.; Miller, J. T.; Meyer, R. J. Correlating the degree of metal-promoter interaction to ethanol selectivity over MnRh/CNTs CO hydrogenation catalysts. *J. Catal.* **2014**, *313*, 149−158); copyright 2014, with permission from Elsevier.

5.3. Ordered Mesoporous Carbon Supported Catalysts. *5.3.1. The Effect of Particle Size and Morphology.* Molybdenum carbide (β-Mo_2C) nanoparticles have been loaded onto a graphitic mesoporous carbon (GMC).[197] GMC appears to be a good support to disperse β-Mo_2C with smaller carbide particles, resulting in higher catalytic activity in HAS from syngas.

An ordered mesoporous carbon nanoparticle (MCN) having a two-dimensional hexagonal structure has been used for HAS from syngas.[198] A Rh/CMK-5-MCN catalyst with a hollow framework configuration exhibited a superior space−time yield for total C_2^+ alcohols when compared with a Rh/CMK-3-MCN with a rod carbon framework. This indicates that the Rh/MCN catalysts exhibited different catalytic activities and selectivities to higher alcohols, which is attributed to the Rh particle size and the accessibility of the reactants to active sites through the morphological effects of the MCNs. Likewise, OMCs with different pore structures (2-D hexagonal and 3-D cubic structures) and different framework configurations (rod-type and hollow-type carbon frameworks) were used to prepare Rh-based catalysts for the catalytic conversion of syngas to alcohols.[199] It was found that these Rh-OMC catalysts exhibited different catalytic activities and selectivities to alcohols, which could be attributed to the size of the metal nanoparticles being confined by the different OMC mesostructures.

5.3.2. The Effect of Promoters. Addition of a minor amount of K_2CO_3 into β-Mo_2C/GMC promoted the formation of higher alcohols (C_2+−OH), leading to a maximum STY for C_2+−OH at a K/Mo ratio of 0.1.[197] Compared with a typical Rh/GMC catalyst promoted three times with Mn, Li, and Fe oxides, the K_2CO_3-promoted β-Mo_2C/GMC catalyst showed higher C_2+−OH selectivity and STY.

5.4. Comparison of Different Shaped Carbon Supported Catalysts. Shaped carbon-supported catalysts have shown higher catalytic activity and alcohol selectivity when compared with oxide-supported catalyst in HAS from syngas,[177,200] which is explained by the difference in the structure of the active phase and in the interaction between these phases and the respective supports. Differently shaped carbons also showed different surface properties and morphology and thus presented different performances for HAS from syngas. For example, the CNT-supported Co−Rh−Mo catalyst showed lower metal dispersion than a similar catalyst supported on commercial ACs.[179] Little or no sintering of metal species was observed on the spent catalyst supported on CNTs, whereas the agglomeration of catalytic species is high on the microporous AC. Likewise, the comparison of β-Mo_2C supported on GMC and commercial carbon materials (AC and CB) showed that the specific rates for CO conversion increased with decreasing carbide particle size, independent of the supports.[197] GMC appears to be a preferable support for β-Mo_2C because of its ability to form smaller carbide particles, resulting in a higher catalytic activity.

In summary, the studies have shown that the properties and morphology of these shaped carbons significantly affected the performance of the catalysts in HAS from syngas. Similar to the discussion in Section 4, novel properties of shaped carbons such as pore-confinement and weak metal−support interaction have been found for shaped carbon-supported catalysts in HAS.[196,199] The effects of promoters, particle size, and pore size are now well documented.

6. CONCLUSIONS, CHALLENGES, AND PERSPECTIVES

The processes that convert syngas to hydrocarbons (FTS) and to alcohols (HAS) have been recognized as important alternative methodologies to produce clean fuels. Both of these reactions require catalysts, preferably supported, and carbon has been found to be useful as a support for both FTS and HAS catalysts. In this Review, we have described the use of various carbon materials that include carbon black (CB), activated carbon (AC), carbon nanotubes (CNTs), carbon nanofibers (CNFs), ordered mesoporous carbon (OMC), carbon spheres (CSs), graphene, and diamond in FTS/HAS studies.

DOI: 10.1021/acscatal.5b00090
ACS Catal. 2015, 5, 2640−2658

In general HAS and FTS catalysts that are placed on *any support* will experience varying metal−support interactions that depend on the support *type*; however, modifying the *shape* of the support can also modify this behavior, and indeed, this has been observed; for example, pore confinement effects in CNTs. Carbons have the advantage that they are easily modified, so these sorts of studies should lead to novel activity/selectivity patterns of products from FTS/HAS that could be related to the support shape.

Some conclusions can be drawn from these studies: (i) Many different carbons have been made, characterized, and used in FTS and HAS studies, especially over the past two decades. The most commonly used carbons studied are those that are readily available, mostly provided by commercial suppliers (ACs, CBs, CSs, CNTs, and CNFs). (ii) All of the above contain small to large amounts of graphene layers/domains, but these sp^2 carbons do not limit sintering in FTS and HAS. (iii) The surfaces of all the carbons are terminated by non-carbon atoms. The number of these atoms will be determined by the carbon domain size. (iv) Further, modification (doping, functionalization) of ALL carbon surfaces is facile, and it is the "defect" sites that are key to contolling catalyst size/sintering/activity and, hence, selectivity. (v) Many FTS studies suggest that because the catalyst particles do not form strong interactions with the carbon support that their activities are higher than found on oxide supports. This relates to the degree of reducibility and the stability of small particles; (vi) Unique features have been found that relate to the use of CNTs in FT and HAS studies. These studies have indicated that there is a difference between the activity/selectivity of metal particles that are placed inside or outside a CNT. This provides a means of adjusting the FT product selectivity. (vii) The role of pores in the carbon supports has been explored; however, in general, carbons with macroscopic pores have been little studied. (viii) There are problems associated with carbons due to their low density and, in some instances, their mechanical strength. Currently, most FT reactors used in industry are packed bed reactors, although various slurry bed and recirculating fluidized beds are also used. When used in a packed bed reactor, a catalyst (of an appropriate size and shape) will need to be pelletized to facilitate mass transfer without too large a pressure drop. This area of study has been little explored and will require further investigation. Thus, the issue of the mechanical strength of pelletized carbon is an issue that could limit the successful industrial application of carbon in FTS (and HAS).

Another issue that will need to be addressed is that many of the pure carbon materials have a low density. Thus, on a volume basis, the number of active sites on a carbon support will be less than on an oxide support, leading to a lower catalytic activity (although on a mass basis, carbon-supported catalysts are competitive). For slurry bed reactors and recirculating fluidized bed catalysts, filtration and abrasion of the catalyst are classical problems associated with metal catalysts. To our knowledge, carbon-supported catalysts have not been tested in a non-fixed-bed-type reactor for FTS to evaluate this issue. Because of the strong mechanical strength of most carbons (e.g., carbon nanotubes), it is unlikely that abrasion will be a problem, provided the metal is strongly anchored to the support. Filtration of the CNTs may be problematic, but this must yet be determined by experiment.

A current limitation on the use of shaped carbons on an industrial scale relates to access and the cost of the carbon support. At present, the carbon supports are expensive, but demand and technology innovation could reduce these costs. However, although the industrial production of CNTs (and CSs and CNFs) is not an issue, access to doped carbons, which will almost certainly be the carbon type of choice, is currently not available on a large scale. Thus, there are a number of challenges that will need to be overcome before carbon supported catalysts can be used in the FTS (and HAS) industry.

AUTHOR INFORMATION

Corresponding Authors

*Phone: 27 11 7176738. Fax: 27 11 7176749. E-mail: Neil.Coville@wits.ac.za.

*E-mail: Haifengxiong@gmail.com.

Notes

The authors declare no competing financial interest.

ACKNOWLEDGMENTS

This work was supported financially by the National Research Foundation of South Africa (NRF) and the University of the Witwatersrand. H. F. Xiong would like to thank the University of the Witwatersrand, Strategy Planning and Resource Allocation Committee (SPARC) for an award of a prestigious postdoctoral fellowship and the Center for Biorenewable Chemicals (CBiRC) supported by NSF Grant EEC-0813570.

REFERENCES

(1) Khodakov, A. Y.; Chu, W.; Fongarland, P. *Chem. Rev.* **2007**, *107*, 1692−1744.

(2) Yue, H.; Ma, X.; Gong, J. *Acc. Chem. Res.* **2014**, *47*, 1483−1492.

(3) Zhang, Q.; Kang, J.; Wang, Y. *ChemCatChem* **2010**, *2*, 1030−1058.

(4) Shaikjee, A.; Coville, N. J. *Small* **2011**, *7*, 2593−2597.

(5) Ebbesen, T. W.; Ajayan, P. M. *Nature* **1992**, *358*, 220−222.

(6) Jung, H. J.; Vannice, M. A.; Mulay, L. N.; Stanfield, R. M.; Delgass, W. N. *J. Catal.* **1982**, *76*, 208−224.

(7) Tau, L. M.; Bennett, C. O. *J. Phys. Chem.* **1986**, *90*, 4825−4832.

(8) Liu, Y.; Luo, J.; Girleanu, M.; Ersen, O.; Pham-Huu, C.; Meny, C. *J. Catal.* **2014**, *318*, 179−192.

(9) Yang, Y.; Chiang, K.; Burke, N. *Catal. Today* **2011**, *178*, 197−205.

(10) Hao, G.-P.; Oschatz, M.; Nickel, W.; Adam, M.; Kaskel, S. *Curr. Org. Chem.* **2014**, *18*, 1262.

(11) Su, D. S.; Perathoner, S.; Centi, G. *Chem. Rev.* **2013**, *113*, 5782−5816.

(12) Zhang, Q.; Cheng, K.; Kang, J.; Deng, W.; Wang, Y. *ChemSusChem* **2014**, *7*, 1251−1264.

(13) Figueiredo, J. L. *J. Mater. Chem. A* **2013**, *1*, 9351−9364.

(14) http://www.carbon-black.org/ International Carbon Black Association.

(15) Donnet, J.-B.; Bansal, R. C.; Wang, M.-J. *Carbon black*, 2nd ed.; Marcel Dekker: New York, 1993.

(16) Xiong, H.; Wang, T.; Shanks, B.; Datye, A. *Catal. Lett.* **2013**, *143*, 509−516.

(17) Marsh, H.; Rodriguez-Reinoso, F. *Activated Carbon*; Elsevier: Amsterdam, London, 2006; pp 1−554

(18) Rodríguez-Reinoso, F. *Carbon* **1998**, *36*, 159−175.

(19) De Jong, K. P.; Geus, J. W. *Catal. Rev.* **2000**, *42*, 481−510.

(20) Serp, P.; Corrias, M.; Kalck, P. *Appl. Catal., A* **2003**, *253*, 337−358.

(21) Iijima, S. *Nature* **1991**, *354*, 56−58.

(22) Jourdain, V.; Bichara, C. *Carbon* **2013**, *58*, 2−39.

(23) Thess, A.; Lee, R.; Nikolaev, P.; Dai, H.; Petit, P.; Robert, J.; Xu, C.; Lee, Y. H.; Kim, S. G.; Rinzler, A. G.; Colbert, D. T.; Scuseria, G. E.; Tománek, D.; Fischer, J. E.; Smalley, R. E. *Science* **1996**, *273*, 483−487.

(24) Ledoux, M. J.; Vieira, R.; Pham-Huu, C.; Keller, N. *J. Catal.* **2003**, *216*, 333−342.

(25) Bezemer, G. L.; Bitter, J. H.; Kuipers, H. P. C. E.; Oosterbeek, H.; Holewijn, J. E.; Xu, X.; Kapteijn, F.; van Dillen, A. J.; de Jong, K. P. *J. Am. Chem. Soc.* **2006**, *128*, 3956−3964.

DOI: 10.1021/acscatal.5b00090
ACS Catal. 2015, 5, 2640−2658

(26) Bezemer, G. L.; Falke, U.; van Dillen, A. J.; de Jong, K. P. *Chem. Commun.* **2005**, *6*, 731−733.
(27) Bezemer, G. L.; Radstake, P. B.; Koot, V.; van Dillen, A. J.; Geus, J. W.; de Jong, K. P. *J. Catal.* **2006**, *237*, 291−302.
(28) Toebes, M. L.; van Heeswijk, J. M. P.; Bitter, J. H.; Jos van Dillen, A.; de Jong, K. P. *Carbon* **2004**, *42*, 307−315.
(29) Díaz, J. A.; Akhavan, H.; Romero, A.; Garcia-Minguillan, A. M.; Romero, R.; Giroir-Fendler, A.; Valverde, J. L. *Fuel Process. Technol.* **2014**, *128*, 417−424.
(30) Asami, K.; Iwasa, A.; Igarashi, N.; Takemiya, S.; Yamamoto, K.; Fujimoto, K. *Catal. Today* **2013**, *215*, 80−85.
(31) Díaz, J. A.; Martínez-Fernández, M.; Romero, A.; Valverde, J. L. *Fuel* **2013**, *111*, 422−429.
(32) Yu, Z.; Borg, Ø.; Chen, D.; Enger, B.; Frøseth, V.; Rytter, E.; Wigum, H.; Holmen, A. *Catal. Lett.* **2006**, *109*, 43−47.
(33) Xiong, H.; Motchelaho, M. A. M.; Moyo, M.; Jewell, L. L.; Coville, N. J. *J. Catal.* **2011**, *278*, 26−40.
(34) Motchelaho, M. A. M.; Xiong, H.; Moyo, M.; Jewell, L. L.; Coville, N. J. *J. Mol. Catal. A: Chem.* **2011**, *335*, 189−198.
(35) Zhang, H.; Chu, W.; Zou, C.; Huang, Z.; Ye, Z.; Zhu, L. *Catal. Lett.* **2011**, *141*, 438−444.
(36) Abbaslou, R. M. M.; Soltan, J.; Dalai, A. K. *Appl. Catal., A* **2010**, *379*, 129−134.
(37) Bahome, M. C.; Jewell, L. L.; Padayachy, K.; Hildebrandt, D.; Glasser, D.; Datye, A. K.; Coville, N. J. *Appl. Catal., A* **2007**, *328*, 243−251.
(38) Chen, W.; Pan, X.; Bao, X. *J. Am. Chem. Soc.* **2007**, *129*, 7421−7426.
(39) Chen, W.; Fan, Z.; Pan, X.; Bao, X. *J. Am. Chem. Soc.* **2008**, *130*, 9414−9419.
(40) Liu, J. J.; Guo, Z.; Childers, D.; Schweitzer, N.; Marshall, C. L.; Klie, R. F.; Miller, J. T.; Meyer, R. J. *J. Catal.* **2014**, *313*, 149−158.
(41) Zhang, H.; Lancelot, C.; Chu, W.; Hong, J.; Khodakov, A. Y.; Chernavskii, P. A.; Zheng, J.; Tong, D. *J. Mater. Chem.* **2009**, *19*, 9241−9249.
(42) Kang, J.; Zhang, S.; Zhang, Q.; Wang, Y. *Angew. Chem., Int. Ed.* **2009**, *48*, 2565−2568.
(43) Lu, J.; Yang, L.; Xu, B.; Wu, Q.; Zhang, D.; Yuan, S.; Zhai, Y.; Wang, X.; Fan, Y.; Hu, Z. *ACS Catal.* **2014**, *4*, 613−621.
(44) Davis, W. R.; Slawson, R. J.; Rigby, G. R. *Nature* **1953**, *171*, 756−756.
(45) Xiong, H.; Motchelaho, M. A. M.; Moyo, M.; Jewell, L. L.; Coville, N. J. *Catal. Today* **2013**, *214*, 50−60.
(46) Shaikjee, A.; Coville, N. J. *Mater. Chem. Phys.* **2011**, *125*, 899−907.
(47) Shaikjee, A.; Coville, N. J. *J. Adv. Res.* **2012**, *3*, 195−223.
(48) Csató, A.; Szabó, A.; Fonseca, A.; Vuono, D.; Kónya, Z.; Volodin, A.; Van Haesendonck, C.; Biro, L. P.; Giordano, G.; Nagy, J. B. *Catal. Today* **2012**, *181*, 33−39.
(49) Serp, P.; Feurer, R.; Kalck, P.; Kihn, Y.; Faria, J. L.; Figueiredo, J. L. *Carbon* **2001**, *39*, 621−626.
(50) Xiong, H.; Pham, H. N.; Datye, A. K. *J. Catal.* **2013**, *302*, 93−100.
(51) Titirici, M.-M. Hydrothermal Carbons: Synthesis, Characterization, and Applications. In *Novel Carbon Adsorbents*; Tascón, J. M. D., Ed.; Elsevier: Oxford, 2012; pp 351−399.
(52) Sun, X.; Li, Y. *Angew. Chem., Int. Ed.* **2004**, *43*, 597−601.
(53) Xia, Y.; Gates, B.; Yin, Y.; Lu, Y. *Adv. Mater.* **2000**, *12*, 693−713.
(54) Deshmukh, A. A.; Mhlanga, S. D.; Coville, N. J. *Mater. Sci. Eng. R: Reports* **2010**, *70*, 1−28.
(55) Xiong, H.; Moyo, M.; Motchelaho, M. A. M.; Jewell, L. L.; Coville, N. J. *Appl. Catal., A* **2010**, *388*, 168−178.
(56) Wang, Z. L.; Kang, Z. C. *J. Phys. Chem.* **1996**, *100*, 17725−17731.
(57) Liang, C.; Li, Z.; Dai, S. *Angew. Chem., Int. Ed.* **2008**, *47*, 3696−3717.
(58) Okazaki, S.; Okuyama, T. *Bull. Chem. Soc. Jpn.* **1983**, *56*, 2159−60.
(59) Rabe, S.; Nachtegaal, M.; Ulrich, T.; Vogel, F. *Angew. Chem., Int. Ed.* **2010**, *49*, 6434−6437.
(60) Jongerius, A. L.; Copeland, J. R.; Foo, G. S.; Hofmann, J. P.; Bruijnincx, P. C. A.; Sievers, C.; Weckhuysen, B. M. *ACS Catal.* **2013**, *3*, 464−473.
(61) Chai, G. S.; Yoon, S. B.; Yu, J.-S.; Choi, J.-H.; Sung, Y.-E. *J. Phys. Chem. B* **2004**, *108*, 7074−7079.
(62) Kelly, K. F.; Billups, W. E. *Acc. Chem. Res.* **2013**, *46*, 4−13.
(63) Nakagawa, K.; Kajita, C.; Ikenaga, N.-o.; Kobayashi, T.; Nishitani-Gamo, M.; Ando, T.; Suzuki, T. *Chem. Lett.* **2000**, *29*, 1100−1101.
(64) Nakagawa, K.; Kajita, C.; Ikenaga, N.-o.; Suzuki, T.; Kobayashi, T.; Nishitani-Gamo, M.; Ando, T. *J. Phys. Chem. B* **2003**, *107*, 4048−4056.
(65) Ovejero, G.; Sotelo, J. L.; Romero, M. D.; Rodríguez, A.; Ocaña, M. A.; Rodríguez, G.; García, J. *Ind. Eng. Chem. Res.* **2006**, *45*, 2206−2212.
(66) Xia, W.; Jin, C.; Kundu, S.; Muhler, M. *Carbon* **2009**, *47*, 919−922.
(67) Tsang, S. C.; Chen, Y. K.; Harris, P. J. F.; Green, M. L. H. *Nature* **1994**, *372*, 159−162.
(68) Omraei, M.; Sheibani, S.; Sadrameli, S. M.; Towfighi, J. *Ind. Eng. Chem. Res.* **2012**, *52*, 1829−1835.
(69) Yook, J. Y.; Jun, J.; Kwak, S. *Appl. Surf. Sci.* **2010**, *256*, 6941−6944.
(70) Girard-Lauriault, P.-L.; Illgen, R.; Ruiz, J.-C.; Wertheimer, M. R.; Unger, W. E. S. *Appl. Surf. Sci.* **2012**, *258*, 8448−8454.
(71) Amiri, A.; Maghrebi, M.; Baniadam, M.; Zeinali Heris, S. *Appl. Surf. Sci.* **2011**, *257*, 10261−10266.
(72) Guczi, L.; Stefler, G.; Geszti, O.; Koppány, Z.; Kónya, Z.; Molnár, É.; Urbán, M.; Kiricsi, I. *J. Catal.* **2006**, *244*, 24−32.
(73) Winter, F.; Leendert Bezemer, G.; van der Spek, C.; Meeldijk, J. D.; Jos van Dillen, A.; Geus, J. W.; de Jong, K. P. *Carbon* **2005**, *43*, 327−332.
(74) Mhlanga, S. D.; Mondal, K. C.; Carter, R.; Witcomb, M. J.; Coville, N. J. *S. Afr. J. Chem.* **2009**, *62*, 67−76.
(75) Couteau, E.; Hernadi, K.; Seo, J. W.; Thiên-Nga, L.; Mikó, C.; Gaál, R.; Forró, L. *Chem. Phys. Lett.* **2003**, *378*, 9−17.
(76) Sidik, R. A.; Anderson, A. B.; Subramanian, N. P.; Kumaraguru, S. P.; Popov, B. N. *J. Phys. Chem. B* **2006**, *110*, 1787−1793.
(77) Czerw, R.; Terrones, M.; Charlier, J. C.; Blase, X.; Foley, B.; Kamalakaran, R.; Grobert, N.; Terrones, H.; Tekleab, D.; Ajayan, P. M.; Blau, W.; Rühle, M.; Carroll, D. L. *Nano Lett.* **2001**, *1*, 457−460.
(78) Xiong, H.; Motchelaho, M. A.; Moyo, M.; Jewell, L. L.; Coville, N. J. *Appl. Catal., A* **2014**, *482*, 377−386.
(79) Motchelaho, M. A. M.; Xiong, H.; Moyo, M.; Jewell, L. L.; Coville, N. J. *J. Mol. Catal. A: Chem.* **2011**, *335*, 189−198.
(80) Li, Y.-H.; Wang, S.; Luan, Z.; Ding, J.; Xu, C.; Wu, D. *Carbon* **2003**, *41*, 1057−1062.
(81) Figueiredo, J. L.; Pereira, M. F. R.; Freitas, M. M. A.; Órfão, J. J. M. *Carbon* **1999**, *37*, 1379−1389.
(82) Jung, H. J.; Walker, P. L., Jr; Vannice, A. *J. Catal.* **1982**, *75*, 416−422.
(83) Martin-Martinez, J. M.; Vannice, M. A. *Ind. Eng. Chem. Res.* **1991**, *30*, 2263−2275.
(84) Moreno-Castilla, C.; Mahajan, O. P.; Walker, P. L., Jr; Jung, H. J.; Vannice, M. A. *Carbon* **1980**, *18*, 271−276.
(85) Jones, V. K.; Neubauer, L. R.; Bartholomew, C. H. *J. Phys. Chem.* **1986**, *90*, 4832−4839.
(86) Sommen, A. P. B.; Stoop, F.; Van Der Wiele, K. *Appl. Catal.* **1985**, *14*, 277−288.
(87) Rodriguez-Reinoso, F.; de Dios López-González, J.; Moreno-Castilla, C.; Guerrero-Ruiz, A.; Rodriguez-Ramos, I. *Fuel* **1984**, *63*, 1089−1094.
(88) Niemantsverdriet, J. W.; Van der Kraan, A. M.; Delgass, W. N.; Vannice, M. A. *J. Phys. Chem.* **1985**, *89*, 67−72.
(89) Kaminsky, M.; Yoon, K. J.; Geoffroy, G. L.; Vannice, M. A. *J. Catal.* **1985**, *91*, 338−351.
(90) Chen, A.; Kaminsky, M.; Geoffroy, G. L.; Vannice, M. A. *J. Phys. Chem.* **1986**, *90*, 4810−4819.
(91) Ma, W.; Kugler, E. L.; Dadyburjor, D. B. *Energy Fuel* **2007**, *21*, 1832−1842.
(92) Ma, W.; Kugler, E. L.; Dadyburjor, D. B. *Energy Fuel* **2011**, *25*, 1931−1938.
(93) Ma, W.; Kugler, E. L.; Wright, J.; Dadyburjor, D. B. *Energy Fuels* **2006**, *20*, 2299−2307.

DOI: 10.1021/acscatal.5b00090
ACS Catal. 2015, 5, 2640−2658

(94) Ma, W.-P.; Ding, Y.-J.; Lin, L.-W. *Ind. Eng. Chem. Res.* **2004**, *43*, 2391−2398.
(95) Ma, W.; Kugler, E. L.; Dadyburjor, D. B. *Energy Fuel* **2010**, *24*, 4099−4110.
(96) Venter, J.; Kaminsky, M.; Geoffroy, G. L.; Vannice, M. A. *J. Catal.* **1987**, *105*, 155−162.
(97) Chen, A. A.; Vannice, M. A.; Phillips, J. *J. Phys. Chem.* **1987**, *91*, 6257−6269.
(98) Ruiz, A. G.; Gonzalez, J. D. L.; Ramos, R. *J. Chem. Soc. Chem. Commun.* **1984**, 1681−1682.
(99) Qian, W.; Zhang, H.; Ying, W.; Fang, D. *J. Nat. Gas Chem.* **2011**, *20*, 389−396.
(100) Qian, W.; Zhang, H.; Ying, W.; Fang, D. *Chem. Eng. J.* **2013**, *228*, 526−534.
(101) Wang, T.; Ding, Y. J.; Xiong, J. M.; Chen, W. M.; Pan, Z. D.; Lu, Y.; Lin, L. W. Fischer−Tropsch reaction over cobalt catalysts supported on zirconia-modified activated carbon. In *Stud. Surf. Sci. Catal.*, Xinhe, B.; Yide, X., Eds.; Elsevier: Amsterdam, 2004; pp 349−354.
(102) Wang, T.; Ding, Y.; Lü, Y.; Zhu, H.; Lin, L. *J. Nat. Gas Chem.* **2008**, *17*, 153−158.
(103) Karre, A. V.; Kababji, A.; Kugler, E. L.; Dadyburjor, D. B. *Catal. Today* **2012**, *198*, 280−288.
(104) Karre, A. V.; Kababji, A.; Kugler, E. L.; Dadyburjor, D. B. *Catal. Today* **2013**, *214*, 82−89.
(105) Den Breejen, J. P.; Radstake, P. B.; Bezemer, G. L.; Bitter, J. H.; Frøseth, V.; Holmen, A.; Jong, K. P. d. *J. Am. Chem. Soc.* **2009**, *131*, 7197−7203.
(106) Den Breejen, J. P.; Sietsma, J. R. A.; Friedrich, H.; Bitter, J. H.; de Jong, K. P. *J. Catal.* **2010**, *270*, 146−152.
(107) Radstake, P. B.; Den Breejen, J. P.; Bezemer, G. L.; Bitter, J. H.; de Jong, K. P.; Frøseth, V.; Holmen, A. On the origin of the cobalt particle size effect in the fischer-tropsch synthesis. In *Stud. Surf. Sci. Catal.*; Fábio Bellot Noronha, M. S.; Eduardo Falabella, S.-A., Eds.; Elsevier: Amsterdam, 2007; pp 85−90.
(108) Trépanier, M.; Dalai, A. K.; Abatzoglou, N. *Appl. Catal., A* **2010**, *374*, 79−86.
(109) Xie, W.; Zhang, Y.; Liew, K.; Li, J. *Sci. Chin. Chem.* **2012**, *55*, 1811−1818.
(110) Chen, W.; Pan, X.; Willinger, M.-G.; Su, D. S.; Bao, X. *J. Am. Chem. Soc.* **2006**, *128*, 3136−3137.
(111) Tavasoli, A.; Trépanier, M.; Dalai, A. K.; Abatzoglou, N. *J. Chem. Eng. Data* **2010**, *55*, 2757−2763.
(112) Abbaslou, R. M. M.; Tavassoli, A.; Soltan, J.; Dalai, A. K. *Appl. Catal., A* **2009**, *367*, 47−52.
(113) Bezemer, G. L.; Radstake, P. B.; Falke, U.; Oosterbeek, H.; Kuipers, H. P. C. E.; van Dillen, A. J.; de Jong, K. P. *J. Catal.* **2006**, *237*, 152−161.
(114) Trépanier, M.; Tavasoli, A.; Dalai, A. K.; Abatzoglou, N. *Appl. Catal., A* **2009**, *353*, 193−202.
(115) Malek Abbaslou, R. M.; Tavasoli, A.; Dalai, A. K. *Appl. Catal., A* **2009**, *355*, 33−41.
(116) Trépanier, M.; Tavasoli, A.; Dalai, A. K.; Abatzoglou, N. *Fuel Process. Technol.* **2009**, *90*, 367−374.
(117) Lv, J.; Ma, X.; Bai, S.; Huang, C.; Li, Z.; Gong, J. *Int. J. Hydrogen Energy* **2011**, *36*, 8365−8372.
(118) van Steen, E.; Prinsloo, F. F. *Catal. Today* **2002**, *71*, 327−334.
(119) Xiong, H.; Zhang, Y.; Wang, S.; Li, J. *Catal. Commun.* **2005**, *6*, 512−516.
(120) Xiong, H.; Zhang, Y.; Liew, K.; Li, J. *J. Mol. Catal. A: Chem.* **2008**, *295*, 68−76.
(121) Xiong, H.; Zhang, Y.; Wang, S.; Liew, K.; Li, J. *J. Phys. Chem. C* **2008**, *112*, 9706−9709.
(122) Borg, Ø.; Eri, S.; Blekkan, E. A.; Storsæter, S.; Wigum, H.; Rytter, E.; Holmen, A. *J. Catal.* **2007**, *248*, 89−100.
(123) Borg, Ø.; Hammer, N.; Eri, S.; Lindvåg, O. A.; Myrstad, R.; Blekkan, E. A.; Rønning, M.; Rytter, E.; Holmen, A. *Catal. Today* **2009**, *142*, 70−77.
(124) Ghampson, I. T.; Newman, C.; Kong, L.; Pier, E.; Hurley, K. D.; Pollock, R. A.; Walsh, B. R.; Goundie, B.; Wright, J.; Wheeler, M. C.; Meulenberg, R. W.; DeSisto, W. J.; Frederick, B. G.; Austin, R. N. *Appl. Catal., A* **2010**, *388*, 57−67.
(125) Hong, J.; Chernavskii, P. A.; Khodakov, A. Y.; Chu, W. *Catal. Today* **2009**, *140*, 135−141.
(126) Lesaint, C.; Glomm, W. R.; Borg, Ø.; Eri, S.; Rytter, E.; Øye, G. *Appl. Catal., A* **2008**, *351*, 131−135.
(127) Liu, Y.; Chen, J.; Fang, K.; Wang, Y.; Sun, Y. *Catal. Commun.* **2007**, *8*, 945−949.
(128) Park, S.-J.; Bae, J. W.; Oh, J.-H.; Chary, K. V. R.; Prasad, P. S. S.; Jun, K.-W.; Rhee, Y.-W. *J. Mol. Catal. A: Chem.* **2009**, *298*, 81−87.
(129) Saib, A. M.; Claeys, M.; van Steen, E. *Catal. Today* **2002**, *71*, 395−402.
(130) Song, D.; Li, J. *J. Mol. Catal. A: Chem.* **2006**, *247*, 206−212.
(131) Liu, Y.; Fang, K.; Chen, J.; Sun, Y. *Green Chem.* **2007**, *9*, 611−615.
(132) Li, B.; Wang, C.; Yi, G.; Lin, H.; Yuan, Y. *Catal. Today* **2011**, *164*, 74−79.
(133) Wang, F.; Wu, H.-Z.; Liu, C.-L.; Yang, R.-Z.; Dong, W.-S. *Carbohydr. Res.* **2013**, *368*, 78−83.
(134) da Conceicao, M. O. T.; Brum, M. C.; dos Santos, D. S.; Dias, M. L. *J. Alloys Compd.* **2013**, *550*, 179−184.
(135) Almarales, A.; Chenard, G.; Abdala, R.; Gomes, D. A.; Reyes, Y.; Tapanes, N. O. *Nat. Sci.* **2012**, *4*, 204−210.
(136) Anilkumar, M.; Hoelderich, W. F. *J. Catal.* **2012**, *293*, 76−84.
(137) Pan, X.; Bao, X. *Acc. Chem. Res.* **2011**, *44*, 553−562.
(138) Bezemer, G. L.; van Laak, A.; van Dillen, A. J.; de Jong, K. P. Cobalt supported on carbon nanofibers- a promising novel Fischer−Tropsch catalyst. In *Stud. Surf. Sci. Catal.*; Xinhe, B.; Yide, X., Eds.; Elsevier: Amsterdam, 2004; pp 259−264.
(139) Torres Galvis, H. M.; Bitter, J. H.; Davidian, T.; Ruitenbeek, M.; Dugulan, A. I.; de Jong, K. P. *J. Am. Chem. Soc.* **2012**, *134*, 16207−16215.
(140) Malek Abbaslou, R. M.; Soltan, J.; Dalai, A. K. *Fuel* **2011**, *90*, 1139−1144.
(141) Bahome, M. C.; Jewell, L. L.; Hildebrandt, D.; Glasser, D.; Coville, N. J. *Appl. Catal., A* **2005**, *287*, 60−67.
(142) Graham, U.; Dozier, A.; Khatri, R.; Bahome, M.; Jewell, L.; Mhlanga, S.; Coville, N.; Davis, B. *Catal. Lett.* **2009**, *129*, 39−45.
(143) Bezemer, G. L.; Remans, T. J.; van Bavel, A. P.; Dugulan, A. I. *J. Am. Chem. Soc.* **2010**, *132*, 8540−8541.
(144) Ma, T.-Y.; Liu, L.; Yuan, Z.-Y. *Chem. Soc. Rev.* **2013**, *42*, 3977−4003.
(145) Ndamanisha, J. C.; Guo, L.-P. *Anal. Chim. Acta* **2012**, *747*, 19−28.
(146) Qiu, S.; Zheng, J.; Yang, G.; Zheng, J.; Wu, M.; Wu, W. *Prog. Chem.* **2014**, *26*, 772−783.
(147) Zhao, C.; Yang, Y.; Wu, Z.; Field, M.; Fang, X.-y.; Burke, N.; Chiang, K. *J. Mater. Chem. A* **2014**, *2*, 19903−19913.
(148) Fu, T.; Jiang, Y.; Lv, J.; Li, Z. *Fuel Process. Technol.* **2013**, *110*, 141−149.
(149) Xiong, K.; Li, J.; Liew, K.; Zhan, X. *Appl. Catal., A* **2010**, *389*, 173−178.
(150) Xiong, K.; Zhang, Y.; Li, J.; Liew, K. *J. Energy Chem.* **2013**, *22*, 560−566.
(151) Sun, B.; Jiang, Z.; Fang, D.; Xu, K.; Pei, Y.; Yan, S.; Qiao, M.; Fan, K.; Zong, B. *ChemCatChem* **2013**, *5*, 714−719.
(152) Honsho, T.-o.; Kitano, T.; Miyake, T.; Suzuki, T. *Fuel* **2012**, *94*, 170−177.
(153) Xiong, H.; Moyo, M.; Rayner, M. K.; Jewell, L. L.; Billing, D. G.; Coville, N. J. *ChemCatChem* **2010**, *2*, 514−518.
(154) Moyo, M.; Motchelaho, M. A. M.; Xiong, H.; Jewell, L. L.; Coville, N. J. *Appl. Catal., A* **2012**, *413−414*, 223−229.
(155) Yu, G.; Sun, B.; Pei, Y.; Xie, S.; Yan, S.; Qiao, M.; Fan, K.; Zhang, X.; Zong, B. *J. Am. Chem. Soc.* **2009**, *132*, 935−937.
(156) Graham, U. M.; Jacobs, G.; Gnanamani, M. K.; Lipka, S. M.; Shafer, W. D.; Swartz, C. R.; Jermwongratanachai, T.; Chen, R.; Rogers, F.; Davis, B. H. *ACS Catal.* **2014**, *4*, 1662−1672.
(157) Fu, T.; Liu, R.; Lv, J.; Li, Z. *Fuel Process. Technol.* **2014**, *122*, 49−57.

DOI: 10.1021/acscatal.5b00090
ACS Catal. 2015, 5, 2640−2658

(158) Xiong, H.; Moyo, M.; Motchelaho, M. A.; Tetana, Z. N.; Dube, S. M. A.; Jewell, L. L.; Coville, N. J. *J. Catal.* **2014**, *311*, 80−87.
(159) Yang, Y.; Jia, L.; Hou, B.; Li, D.; Wang, J.; Sun, Y. *ChemCatChem* **2013**, *6*, 319−327.
(160) Nakamura, J.; Kondo, T. *Top. Catal.* **2013**, *56*, 1560−1568.
(161) Han, Z.; Fina, A. *Prog. Polym. Sci.* **2011**, *36*, 914−944.
(162) Hepplestone, S. P.; Ciavarella, A. M.; Janke, C.; Srivastava, G. P. *Surf. Sci.* **2006**, *600*, 3633−3636.
(163) Kim, P.; Shi, L.; Majumdar, A.; McEuen, P. L. *Phys. Rev. Lett.* **2001**, *87*, 215502.
(164) Liu, Y.; Ersen, O.; Meny, C.; Luck, F.; Pham-Huu, C. *ChemSusChem* **2014**, *7*, 1218−1239.
(165) Riccardis, M. F. D.; Carbone, D.; Makris, T. D.; Giorgi, R.; Lisi, N.; Salernitano, E. *Carbon* **2006**, *44* (4), 671−674.
(166) Zarubova, S.; Rane, S.; Yang, J.; Yu, Y.; Zhu, Y.; Chen, D.; Holmen, A. *ChemSusChem* **2011**, *4*, 935−942.
(167) Liu, Y.; Dintzer, T.; Ersen, O.; Pham-Huu, C. *J. Energy Chem.* **2013**, *22*, 279−289.
(168) Torres Galvis, H. M.; Bitter, J. H.; Khare, C. B.; Ruitenbeek, M.; Dugulan, A. I.; de Jong, K. P. *Science* **2012**, *335*, 835−838.
(169) Yu, Z.; Borg, Ø.; Chen, D.; Enger, B.; Frøseth, V.; Rytter, E.; Wigum, H.; Holmen, A. *Catal. Lett.* **2006**, *109*, 43−47.
(170) Zaman, M.; Khodadi, A.; Mortazavi, Y. *Fuel Process. Technol.* **2009**, *90*, 1214−1219.
(171) Wu, Q.; Christensen, J. M.; Chiarello, G. L.; Duchstein, L. D. L.; Wagner, J. B.; Temel, B.; Grunwaldt, J.-D.; Jensen, A. D. *Catal. Today* **2013**, *215*, 162−168.
(172) Yeon, S. H.; Shin, D. H.; Nho, N. S.; Shin, K. H.; Jin, C. S.; Nam, S. C. *Korean J. Chem. Eng.* **2013**, *30*, 864−870.
(173) Lu, Z.; Tang, H. D.; Liu, C. L.; Liu, H. Z. *Chin. J. Catal.* **2011**, *32*, 1250−1255.
(174) Li, X. G.; Feng, L. J.; Zhang, L. J.; Dadyburjor, D. B.; Kugler, E. L. *Molecules* **2003**, *8*, 13−30.
(175) Iranmahboob, J.; Hill, D. O. *Catal. Lett.* **2002**, *78*, 49−55.
(176) Li, X. G.; Feng, L. J.; Liu, Z. Y.; Zhong, B.; Dadyburjor, D. B.; Kugler, E. L. *Ind. Eng. Chem. Res.* **1998**, *37*, 3853−3863.
(177) Surisetty, V. R.; Eswaramoorthi, I.; Dalai, A. K. *Fuel* **2012**, *96*, 77−84.
(178) Jiao, G. P.; Ding, Y. J.; Zhu, H. J.; Li, X. M.; Li, J. W.; Dong, W. D.; Pei, Y. P. *Chin. J. Catal.* **2009**, *30*, 825−829.
(179) Surisetty, V. R.; Dalai, A. K.; Kozinski, J. *Appl. Catal., A* **2011**, *393*, 50−58.
(180) Wang, S. R.; Guo, W. W.; Wang, H. X.; Zhu, L. J.; Qiu, K. Z. *Catal. Lett.* **2014**, *144*, 1305−1312.
(181) Zhang, H. B.; Dong, X.; Lin, G. D.; Liang, X. L.; Li, H. Y. *Chem. Commun.* **2005**, *40*, 5094−5096.
(182) Liang, X.-L.; Dong, X.; Li, H.-Y.; Lin, G.-D.; Zhang, H.-B. *Xiamen Daxue Xuebao (Ziran Kexue Ban)* **2005**, *44*, 445−449.
(183) Ma, C.-H.; Li, H.-Y.; Lin, G.-D.; Zhang, H.-B. *Catal. Lett.* **2010**, *137*, 171−179.
(184) Wang, J.-J.; Xie, J.-R.; Huang, Y.-H.; Chen, B.-H.; Lin, G.-D.; Zhang, H.-B. *Appl. Catal., A* **2013**, *468*, 44−51.
(185) Ma, X. M.; Lin, G. D.; Zhang, H. B. *Chin. J. Catal.* **2006**, *27*, 1019−1027.
(186) Tavasoli, A.; Karimi, S.; Nikookar, H.; Fadakar, H. *Iranian J. Chem. Chem. Eng., Int. Engl. Ed.* **2013**, *32* (1), 11−19.
(187) Tavasoli, A.; Karimi, S.; Davari, M.; Nasrollahi, N.; Nematian, T. *J. Ind. Eng. Chem.* **2014**, *20*, 674−681.
(188) Surisetty, V. R.; Kozinski, J.; Dalai, A. K. *Int. J. Chem. Reactor Eng.* **2011**, *9*, 1−18.
(189) Shi, L. M.; Chu, W.; Deng, S. Y. *J. Nat. Gas Chem.* **2011**, *20*, 48−52.
(190) Boahene, P. E.; Surisetty, V. R.; Sammynaiken, R.; Dalai, A. K. *Top. Catal.* **2014**, *57*, 538−549.
(191) Ma, C. H.; Li, H. Y.; Lin, G. D.; Zhang, H. B. *Appl. Catal., B* **2010**, *100*, 245−253.
(192) Wu, X. M.; Guo, Y. Y.; Zhou, J. M.; Lin, G. D.; Dong, X.; Zhang, H. B. *Appl. Catal., A* **2008**, *340*, 87−97.
(193) Wu, X.-M.; Guo, Y.-Y.; Li, H.; Lin, G.-d.; Zhang, H.-b. *Xiamen Daxue Xuebao (Ziran Kexue Ban)* **2007**, *46*, 445−450.
(194) Surisetty, V. R.; Dalai, A. K.; Kozinski, J. *Appl. Catal., A* **2010**, *381*, 282−288.
(195) Surisetty, V. R.; Dalai, A. K.; Kozinski, J. *Appl. Catal., A* **2010**, *385*, 153−162.
(196) Pan, X.; Fan, Z.; Chen, W.; Ding, Y.; Luo, H.; Bao, X. *Nat. Mater.* **2007**, *6*, 507−511.
(197) Chai, S. H.; Schwartz, V.; Howe, J. Y.; Wang, X. Q.; Kidder, M.; Overbury, S. H.; Dai, S.; Jiang, D. E. *Microporous Mesoporous Mater.* **2013**, *170*, 141−149.
(198) Kim, M. J.; Chae, H. J.; Ha, K. S.; Jeong, K. E.; Kim, C. U.; Jeong, S. Y.; Kim, T. W. *J. Porous Mater.* **2014**, *21*, 365−377.
(199) Kim, M. J.; Chae, H. J.; Ha, K. S.; Jeong, K. E.; Kim, C. U.; Jeong, S. Y.; Kim, T. W. *J. Nanosci. Nanotechnol.* **2013**, *13*, 7511−7518.
(200) Li, Z. R.; Fu, Y. L.; Jiang, M.; Hu, T. D.; Liu, T.; Xie, Y. N. *J. Catal.* **2001**, *199*, 155−161.
(201) Lu, G.; Zhang, C. F.; Gang, Y. Q.; Zhu, Z. B.; Ni, Y. H.; Cheng, L. J.; Yu, F. *Appl. Catal., A* **1997**, *150*, 243−252.
(202) Feng, L. J.; Li, X. G.; Dadyburjor, D. B.; Kugler, E. L. *J. Catal.* **2000**, *190*, 1−13.
(203) Tavasoli, A.; Karimi, S.; Zolfaghari, Z.; Taghavi, S.; Amirfirouzkouhi, H.; Babatabar, M. *Iranian J. Chem. Chem. Eng.-Int. Engl. Ed.* **2013**, *32*, 21−29.
(204) Peng, W.; Wang, Q. W.; Jiang, B.; Ji, P. J. *Ind. Eng. Chem. Res.* **2011**, *50*, 11067−11072.

DOI: 10.1021/acscatal.5b00090
ACS Catal. 2015, 5, 2640−2658